ENDOPLASMIC RETICULUM DYNAMICS, FORM, AND CYTOSKELETAL ASSOCIATION CHANGES DURING PLASMOLYSIS – DEPLASMOLYSIS CYCLE

A Thesis

by

XIAOHANG CHENG

Submitted to the Office of Graduate and Professional Studies of
Texas A&M University
in partial fulfillment of the requirements for the degree of

MASTER OF SCIENCE

Chair of Committee,	Lawrence Griffing
Committee Members,	Wayne Versaw
	Brian Shaw
Head of Department	Thomas McKnight

August 2016

Major Subject: Biology

ABSTRACT

Endoplasmic reticulum (ER), as the largest endomembrane system in eukaryotic cells, plays important roles in material synthesis and distribution. However, the underlying function of this amazing network in relation to the rest of the cell is largely unknown. In our studies, we use plasmolysis as a tool to study the shape and dynamics change of endoplasmic reticulum. During the process of plasmolysis, the portion of ER that remains in the protoplast goes through dramatic shape and dynamic change, which can be quantified using persistency mapping. Together with fluorescence recovery after photo-bleaching (FRAP) analysis, we found that accompanying the shrinkage of the protoplast and its retraction from the cell wall, the protoplast endoplasmic reticulum becomes more persistently cisternalized without changing its association with the cytoskeleton or its internal flow. On the other hand, as the protoplast pulls away from the inside surface of cell wall during plasmolysis, the volume of protoplast shrinks, while leaving parts of the ER and cytoskeletal components in the periplasmic region, forming Hechtian strands and the Hechtian reticulum that remain attached to the cell wall. The portion of ER that remains attached to the cell wall forms Hechtian strands and the Hechtian reticulum, and they have decreased internal flow and become more tubular shaped. For Hechtian reticulum specifically, it co-localizes with microtubule. 3D reconstruction models based on fluorescent confocal live images reveal the detailed structure and spatial organization of ER, plasma membrane and cell wall within the periplasmic region, as well as the ER – microtubule co-localization in the Hechtian reticulum. Interestingly, we found that within the periplasmic region, plasma membrane do not retract from the vicinity of the inner surface of the cell wall as protoplast is pulling away. Instead it forms a cover at the region where Hechtian reticulum forms. Together, our model suggests that the formation sites of Hechtian reticulum and Hechtian strands are potential cell wall – plasma membrane – ER anchor points. These anchor points may have important functions in ER morphological and dynamic control, thus contributing to biological processes from nutrition and growth to pathogen defense during the life span of plants.

TABLE OF CONTENTS

LIST OF FIGURES

CHAPTER I

INTRODUCTION

The classic model of endoplasmic reticulum

Endoplasmic reticulum (ER), as the largest endomembrane system in eukaryotic cells, plays important roles in intracellular material synthesis and distribution. In most types of eukaryotic cells, about half of the total area of membrane in a eukaryotic cell consists of ER membrane (*1*). This large membrane surface provides platform for intracellular material (like proteins and lipids) synthesis and sorting. In classical descriptions based on electron microscopy, ribosomes have been seen attached to the cytosolic surface of endoplasmic reticulum, thus the portion of ER that has ribosome attached to it is called rough ER. “Rough sheets and smooth tubules” have been described in yeast and mammalian cells (*2-4*). Those two types of ER components have different functions, with rough ER (mainly in tubular form) being the regions of co-translational insertion and smooth ER (mainly in cisternal form) being sites of lipid biosynthesis.

However, the underlying function of this amazing network organization in relation to the rest of the cell is largely unknown. Recent studies on ER interactions with plasma membrane (primarily through membrane contact sites – MCS’s) (*5-8*) and other organelles including mitochondria (*9*) and chloroplasts (*10*) indicate novel intra-cellular pathways of material transport and signal transduction. Studies regarding ER – cytoskeleton interactions indicate potential mechanisms of ER shape and dynamics control (*11, 12*), which may also directly or indirectly influence cytoplasmic streaming and luminal protein flow (*13*). How these interactions relate to the function and shape control of the ER remains a largely unanswered question.

Endoplasmic reticulum structure and its regulation

In eukaryotes, the endoplasmic reticulum (ER) is a membrane-bound organelle that has a finely articulated and highly dynamic polygonal network (Figure 1-1). The basic morphological components of ER were described as arrays of tubules and sheet-like

cisternae (*14*), as well as the specifically differentiated subdomains such as the highly curved nuclear envelope. Most of the intracellular space is occupied with the central vacuole in plants, but even within the narrow space defined by the tonoplast and plasma membrane, the majority of the ER is located in the cortical part of the cell adjacent to the plasma membrane and cell wall, and is thus called cortical endoplasmic reticulum (Figure 1-1 A). There is also abundant internal ER, particularly in secretory and tip-growing cells where there is a large separation between the tonoplast and plasma membrane. The internal portion of ER ramifies through the cell, often connected with other organelles through membrane contact sites (MCSs), and in highly vacuolate cells, it can be found within trans-vacuolar strands. This ER network forms a single compartment with a continuous intraluminal space contoured by a continuous membrane (*15*).

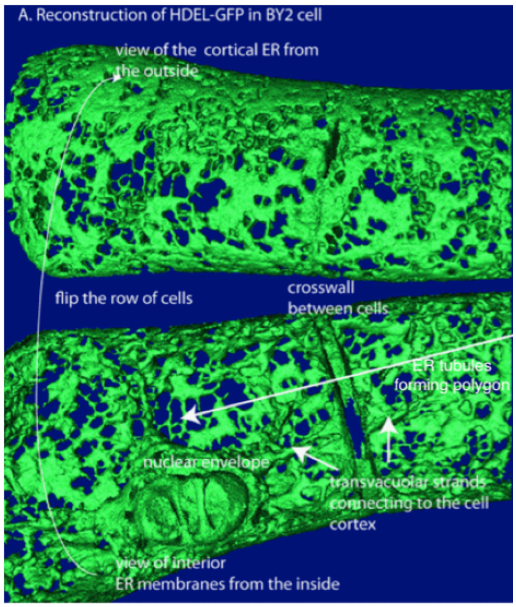

Figure 1-1. ER organization in plant cells. A) 3D reconstructions of ER with GFP marked in its lumen in BY2 cells (*16*). ER tubules, cisternae and nuclear envelope can be seen. B) ER of *Nicotiana benthamiana* seedlings at 8 min in 0.75M D-sorbitol hyperosmotic treatment, ER still have fine polygonal organization. D) ER of *N. benthamiana* seedlings at 49 min in 0.75M D-sorbitol hyperosmotic treatment, large cisternae appeared (*17*). C) Largely cisternalized ER in *Arabidopsis* root meristematic cells. E) Tubularized ER in elongated *Arabidopsis* root epidermal cells (*18*).

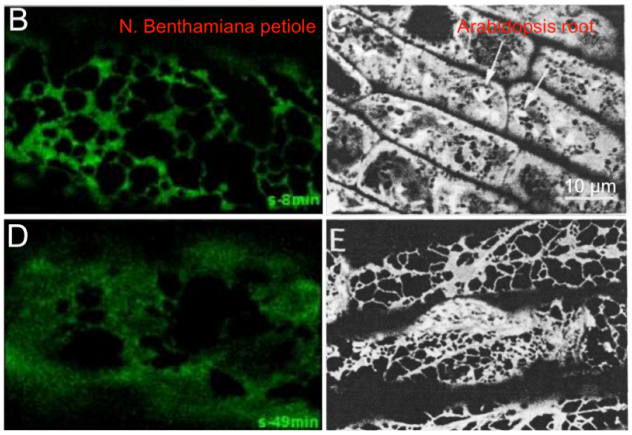

Figure 1-1 Continued.

The diameter of the ER tubules is about 30 nm in yeast and 50 nm in mammals (*19*), and 50-60 nm (*20*) in plant cells. This is also the luminal thickness of ER cisternae, therefore the edges of cisternae have the same level of curvature as ER tubules (*19*). The limits of the ER sheet width may be determined by climp63 in mammalian cells (*19*), but the determinants of cisternal thickness in plants and fungal cells are not known. The ER tubule is stabilized, and perhaps generated, through the activities of those families of curvature-stabilizing proteins including reticulons and DP1/Yop1p (*21-23*), and which are present in both tubule and the high curvature edges of cisternae (*19*). Extreme examples of highly tubular ER can be found in desmotubules formed inside the plasmodesmata, which connect plant cells by extending across the cell wall. The desmotubule has an even smaller diameter, which is around 15 nm (*24*).

The classic model for ER interaction with other membrane-bound organelles (mainly Golgi apparatus) is through vesicular trafficking. However more recent studies on ER – Golgi tethering interactions indicate direct contact of ER and Golgi apparatus (*25*). This interaction was suggested to be one type of moving force for organelle streaming, and was also hypothesized to allow transport of cargo from the ER to Golgi via Golgi attached export sites (*26*). Other studies of ER interaction with highly movable organelles such as peroxisomes and mitochondria also support the idea that the communication of the ER with other organelles is not restricted to only vesicular trafficking (*8*). For ER interactions with less movable organelles, ER was also observed

to form a ring around the cleavage planes of the chloroplast during chloroplast division (Griffing, unpublished), and forms a hammock-like nexus that surround the non-dividing chloroplast in the plant cell (*10*). There are also clear close contacts (MCS's) between the ER and plasma membrane in plants (*7*).These associations with other organelles also indicate that it may serve as a potential organizer of smaller organelles (Figure 1-2). The spatial organization of these other organelles has often been thought to be the province of the cytoskeleton. In the experiments described below, we show that there is interplay among the ER, the cell wall, and the cytoskeleton in the spatial organization of the cell. The process of plasmolysis provides a unique opportunity to observe this interplay.

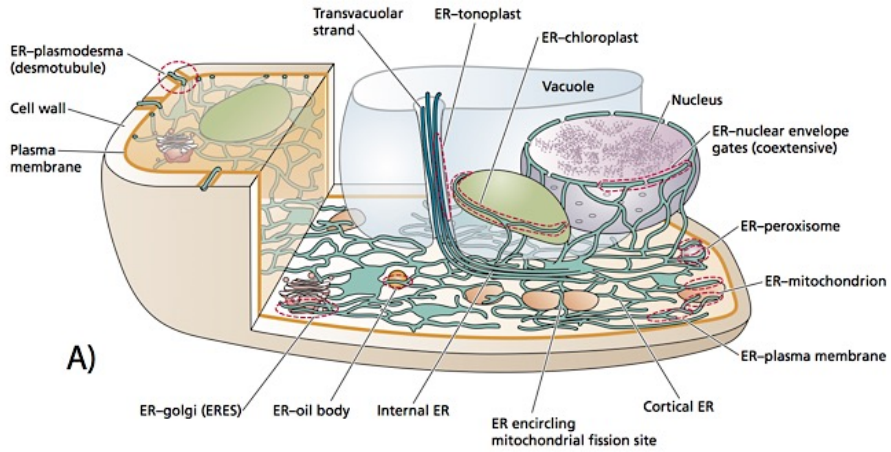

Figure 1-2. Representations for the general ER structures within plant cells. Cortical ER with cisternal and tubular network is shown, anchor points to the cell wall and interaction with other organelles are described (*27*).

Endoplasmic reticulum dynamics

The ER network is not stationary. Instead it is constantly going through different types of movement. Different domains of ER that have different shapes connect to each other while constantly undergoing shape change, which is usually called remodeling. Together with remodeling there is also translational movement or displacement, which

involves both of the membrane and luminal component moving together. Previous studies on the ER network in *tobacco* leaf epidermal cells indicate that ER network does not move by global shifting of cisternae or tubular polygons. Instead, the movement is achieved through network remodeling (*11, 12*). Network remodeling involves shape changing of tubule and cisternae, usually growing and fusing of tubules and filling or fenestration of cisternae (*3, 16*). All this movement involves ER membrane fusion. Proteins like Rab10 (*28*) have been identified to play important rolls in ER tubule growth and fusion in animal cells, and some other ER membrane proteins like RHD3 in *Arabidopsis thaliana* and its functional homolog in mammals, atlastin, and yeast, SEY1p, have been implicated in homotypic fusion of ER membrane (*29-31*).

Besides remodeling and translational movements, both plant ER membrane and lumen proteins are diffusively and, in some cases, advectively flowing. Photo-activation studies use ER membrane localized protein calnexin trans-membrane domain fused with photo-activatable GFP showed that ER membrane proteins are advectively flowing (*12, 32*). Optic-flow based analysis of flow using plant lines with ER lumen labeled with GFP indicate that the rapidly moving regions, the fast lanes, of ER have advective flow, and this flow is thought to be primarily driven by myosin XI-K (*13*). The presence of non-homogeneous advective and diffusional flows in the network, superimposed on the remodeling of the network itself presents the challenge of determining what are the main contributors to each type of flow, including lumenal and surface (membrane) flow. In this study, we map the luminal flows using FRAP and a combination of luminal flow and remodeling using simple optic flow analysis in different regions of the ER.

Plasmolytic dynamics and ER behavior during plasmolysis

Plasmolysis is a physiological event that occurs in plant cells under severe osmotic stress (*33*). As the plant cell loses turgor pressure in hyperosmotic external solutions, water comes out from the cell primarily from inside the vacuole. The protoplast pulls away from the inside surface of cell wall and as a result, the volume of protoplast shrinks (*34*). This process is reversible. Once the plant cell is exposed to a hypotonic solution, water comes back inside the protoplast and increases its volume until the protoplast is fully expanded and abutted against the inner lining of the cell wall.

The region where protoplast shrinks away from the cell wall is known as the periplasmic space (*35*). Strand-like structures in the periplasmic space that connect the withdrawn protoplast to the cell wall were characterized in 1912 by Hecht (*36*), and are called Hechtian strands. Later studies with $DiOC_6$ staining for fluorescent microscopy and phosphotungstic acid (PTA) staining for electron microscopy, Hechtian strands were identified as tubule structures with a diameter about 50 nm to 100 nm (Figure 1-3 A) (*37*). The tubules were made of double membrane, with the inner membrane hypothesized to be $DiOC_6$-stained ER membrane and outer membrane as phosphotungstic acid-stained plasma membrane (*37*). Besides Hechtian strands, another form of tubule network, again hypothesized to contain, but not yet shown to be ER, is also present and attached to the inner surface of the cell wall within the periplasmic space. It is called the Hechtian reticulum (reticulation) (Figure 1-3 B) (*38*). $DiOC_6$-stained mitochondria were also observed to be in Hechtian strands in some occasions (*39*). Together with the fact that $DiOC_6$ can be a non-specific stain, the presence of $DiOC_6$-stained membranes in the Hechtian reticulum or Hechtian strands is not an unequivocal demonstration of the presence of ER (*40*). Some, but not all, of the anchoring sites of Hechtian strands on the cell wall were identified as desmotubules in plasmodesmata (*37*).

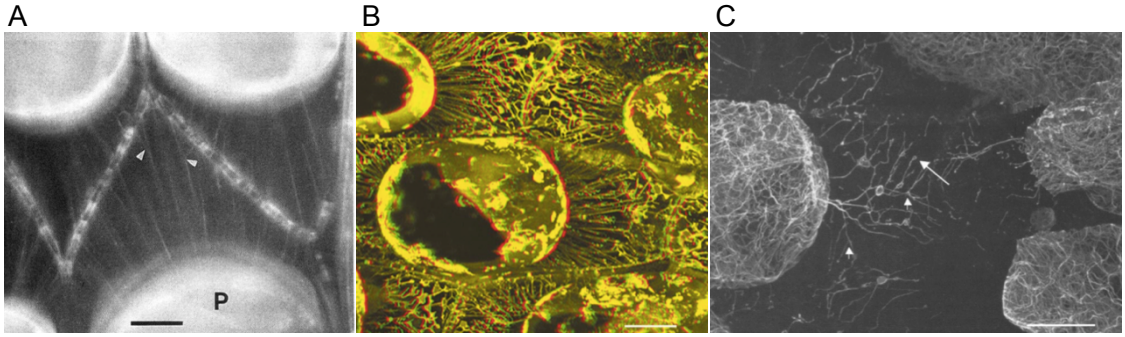

Figure 1-3. Hechtian strands, Hechtian reticulum, and cytoskeleton present within periplasmic region. A) Hechtian strands stained by $DiOC_6$ in onion epidermal cells, bar = 30 µm (*37*) B) Hechtian strands (straight) and reticulum (branched) stained by $DiOC_6$ in onion epidermal cells, bar = 50 µm (*38*). C) Immunofluorescence of the microtubule cytoskeleton present in the periplasmic region with antibody staining, bar = 20 µm (*39*).

Interestingly, not only are membrane-bound tubular structures present within the periplasmic region, but also cytoskeleton is observed there. Curved strands of microtubule also remained in the periplasmic region and appeared to be a branching network (Figure 1-3 C), with one end appearing to be attached to the protoplast. ER, known to be having interactions with cytoskeleton within the cytoplasm (*12*), may change its spatial relationship with cytoskeleton and flow dynamics upon plasmolysis. This approach of isolating periplasmic ER may reveal important facts about how ER motility, flows, and shape maintenance are linked to cytoskeletal and plasma membrane-wall interactions. The persistent association of organelles with the cell wall and plasma membrane within the periplasmic region while the protoplast pulls away from it may reveal important information about the nature of organelle anchoring to the plasma membrane and the cell wall.

CHAPTER II

ER SHAPE AND CYTOSKELETAL ASSOCIATION CHANGE DURING PLASMOLYSIS

Introduction

In elongating petioles and expanding leaf pavement cells, the dynamics of the ER arise through its interaction with actin and myosin (*12, 13*). The dynamics diminish considerably in the presence of latrunculin b, a filamentous actin de-polymerization agent. Meanwhile there is a small amount of remaining ER movement that occurs on microtubules, presumably through ER membrane anchoring proteins (*8, 41*). These cortical microtubule association regions may also be associated with membrane contact sites, since some of the proteins of membrane contact sites are microtubule binding proteins (*5, 8*), however clear evidence for the association of microtubules with membrane contact sites is lacking. Earlier work has shown that a microtubule network resides in fixed cells within the region where Hechtian reticulum is present, Figure 1-3 C (*39*), but the association with the ER was not determined. Other work indicates that the Hechtian reticulum is actin-poor, while the Hechtian strands are actin-rich (*35*), but again, the presence of the ER and its dynamics in this region has not been investigated with specific ER markers.

In this chapter, two of the questions we address are: 1) Does the Hechtian reticulum contain ER and branched microtubules in the same region of periplasmic space? And 2) Do the ER and microtubules have the kind of branching structure which is different from the standard organization of microtubules? If co-localization of the ER and microtubules occurs within periplasmic space, this may potentially identify the portion of ER that is associated with microtubule. And because of its stationary feature while protoplast pulls away and its close affinity toward cortical cell wall, it may reveal mechanisms for cortical ER organization at the cell periphery. The formation of Hechtian reticulum and Hechtian strands may indicate regions where the ER and the PM are anchored to the cell wall. We hypothesize that these anchor sites, or MCS's (*5, 7, 8*), generate the less movable

part of cortical ER and provide “control points” to maintain the polygonal network configuration of the ER (Figure 1-2).

Here we approach these problems with analysis of the shape changes of ER during plasmolysis by using 3D reconstruction based on confocal images of stable transgenic plant lines with ER lumen specific label, GFP-HDEL to visualize protoplast ER and periplasmic ER within Hechtian strands and reticulum. When examining the organization of the cytoskeleton in relation to the ER and its plasma membrane MCS’s we used stable transgenic lines double-labeled with mCherry-HDEL and either GFP-labeled tubulin (GFP-TUA) or YFP-labeled fibrin actin-binding domain (YFP2-FABD). Co-localization was analyzed in 2D and using 3D reconstruction. To determine the polymerization state and/or presence of movement of the polymers of microtubules present in the periplasmic region, fluorescence recovery after photo-bleaching (FRAP) analysis was used. Periplasmic microtubules are extensively branched, thereby differing considerably from normal cytoplasmic microtubules that are less frequently branched (either at the site of new polymerization of microtubules or cleavage of pre-existing microtubules). The dynamics of microtubule may indicate its function, revealing whether or not it serves as a track for ER.

Materials and methods

1. Transgenic plant growth and plasmolysis experiment

Plants were cultured in petri dishes that contain half-strength MS media with 1 % (w/v) agar, at room temperature in 17.5-hour days. *Nicotiana benthamiana* and *Arabidopsis thaliana* seedlings between 1 – 2 weeks old were used for live imaging. To obtain z-stacks for 3D reconstruction that characterizes the shape changes of ER, *Nicotiana benthamiana* line 16c (*42, 43*) constitutively expresses GFP-HDEL labeling the ER lumen was used.

For the experiments characterizing co-localization of Hechtian strand and reticulum with cytoskeleton, transgenic plants constitutively express 35S: YFP-ABD2-YFP (Ex: 514 nm Em: 527 nm) labeling Actin microfilaments (courtesy of Elison Blancaflor, Noble

Foundation, Ardmore, OK, USA) and GFP-Tua6 (Ex: 488 nm Em: 510 nm) labeled alpha tubulin (courtesy of Ueda et al (*44*)) are transformed with STS-mCherry-HDEL (Ex: 587 nm Em: 610 nm) by agrobacterium mediated T-DNA insertion respectively, creating ER-Microfilament and ER-Microtubule double labeled lines. Seedlings expressing both types of fluorescence were screened and cultured after screening the T2 generation of the transformed plants. Individuals expressing strong fluorescence in T2 generation were screened right before being imaged for Hechtian strand – cytoskeleton co-localization. For microtubule photo-bleaching experiment, both ER-microtubule double-labeled line and its parent line with GFP-TUA6 labeling were used.

Plasmolysis experiment was carried out between normal glass slide and coverslip. Plant seedlings were mounted in 10 mM 2-(N-morpholino) ethanesulfonic acid (MES) buffer (pH 5.8) and imaged for control under non-osmotic shock environment. MES buffer was then removed carefully by sticking thin slices of Kimwipes (Kimtech Science, USA) between slides and coverslip to absorb the liquid. Plasmolyticum (0.75M sorbitol in 10mM MES solution, pH 5.8) was then added between slide and coverslip till the seedling was fully immersed. Seedlings goes through obvious shrinkage during the first 15 min of hypertonic solution treatment, which will cause focal plane of interest to get out of focus if not adjusted over several minutes. To minimize seedling shrinkage derived frame shifting and loss of focus, petri dishes (Fisherbrand, USA) with a rectangular opening in the center covered by a rectangular coverslip was used for inverted microscope. A seedling is placed on top of the coverslip with another coverslip on top of it to create a “sandwich” with the seedling and the plasmolyticum (or buffer for control) in the center. This significantly diminished shifting or losing focus and created a stable imaging environment.

2. Fluorescent dye labeling

For periplasmic region labeling, 2.5 mg/mL Lucifer yellow was included in the plasmolyticum. Seedlings expressing GFP-HDEL were treated for 45 min in 0.75 M sorbitol solution in 10 mM MES buffer to achieve stable plasmolysis while imaging with confocal microscopy for monitoring protoplast withdrawing. Then the same seedling was transferred into sorbitol plus 2.5 mg/mL lucifer yellow before putting it back for

confocal imaging. Lucifer yellow was excited with the same 488 nm argon laser that was used to view ER luminal GFP, and emission light is also collected at the same wavelength (Ex: 488 nm Em: 510 nm). The intensity of Lucifer yellow is weaker compare to the bright ER network, thus it can stand out from the GFP fluorescence within the ER lumen.

To label the plasma membrane, 20 μM/L FM4-64 dye (Ex: 515 nm Em: 640 nm) was included in plasmolyticum during plasmolysis experiments and excited with 543nm argon laser. For cell wall labeling, seedlings were soaked in 10μg/mL propidium iodide (PI, Ex: 535 nm Em: 617 nm) for 15 min before transfer into plasmolyticum. *Nicotiana benthamiana* seedlings constitutively expressing GFP were imaged with both channels for the two types of fluorescence in order to get 3D reconstruction for both ER and plasma membrane.

3. 3D reconstruction

Fluorescent live images were acquired using Olympus FV1000 laser scanning confocal microscope with a NA 1.2 UPLSAPO water immersion 60X objective, and inverted Olympus IX81 laser spinning-disc confocal microscope with either 40× (NA 1.3) or 100 × (NA 1.53) oil immersion objective. Z-stack images for 3D reconstruction were taken on Olympus FV1000 laser scanning confocal microscope with a 1.2NA UPLSAPO water immersion 60X objective, with a step size of half of the Z-resolution. Pixel size was adjusted to fit the Nyquist criterion and pixel dwell time was adjusted to maximize fluorescence while maintaining fast scanning speed. 3D images were generated using surface rendering with the ImageJ 3D viewer pluggin in ImageJ (*45*) and the open source software package, Visualization Tool Kit (VTK) (*46*) as described in Enloe and Griffing, (2000) (*47*). Images of 3D reconstructed structures were later exported as tiff files and edited in Adobe illustrator (*48*) for labeling and annotation.

4. Fluorescence recovery after photo-bleaching (FRAP) analysis

Photobleaching of microtubule during plasmolysis was carried out in Olympus FV1000 laser scanning confocal microscope by using a 405 nm diode laser that was set to

100% transmission. A 20-frame (53X53 μm^2, 200X200 $pixel^2$) video was taken for each bleaching event, with a frame interval 0.8 seconds. Bleach start after recording first 5 frames in a circular inset (diameter about 20 pixel) ROI, lasting total 368.64 ms. For FRAP analysis, all frames of the videos were acquired as 16-bit gray-scale images. Each analyzed video was first processed with Image stabilizer plugin of ImageJ (*49*). A polygon that selected only the cell being bleached is created manually and added to ROI manager to be used for normalization. FRAP analysis was then carried out using FRAP profiler final plugin in (*50*). Recovery halftime and percent (%) mobility was collected from each image and used for statistical analysis. Statistical analysis was carried out using JMP software. Both recovery halftime and percent mobility from each microtubule component (polymerized microtubule in normal cytoplasm, depolymerized microtubule in protoplast and microtubule component in Hechtian reticulum) are first compared by one-way ANOVA analysis, then compared by pairs using Tukey-Kramer HSD analysis. For both analyses the confidence level is 95% ($p<0.05$).

Results

1. Protoplast ER becomes more cisternalized during plasmolysis and recovery

In order to observe the morphological change of endoplasmic reticulum during plasmolysis, intact seedlings of ER-HDEL labeled *N. benthamina* were used for confocal live imaging. Cortical ER of a single hypocotyl cell (approximately the fifth cell from root-shoot junction along the stem) was used for all the experiments (Figure 2-1, dark green facet on the surface of the cell (right panel) represents the cortical cell wall). Obvious shrinking of the entire seedling was seen within a few minutes of plasmolyticum addition and became more stable after obvious plasmolysis started to happen. Before the protoplasts started to retract from the cell wall, cells seem to be "flattened" because of the loss of turgor pressure (Figure 2-2 C and 2-3).

ER within the protoplasts continued to cisternalize as the plasmolysis went on. As seen in Figure 2-2 A, control cells have fine cortical ER network with thin tubules articulate with each other, few cisternae are seen at some of the tubule junctions. Distinct Hechtian strands and reticulum formations were usually seen after 45 min of

plasmolyticum treatment (Figure 2-2 C), what accompanies it is increasing cisternalization. While in Figure 2-2 B, when the plant cell regains turgor following plasmolysis, some of the mesh seemed to fuse together to form more cisternae. This recovery period is defined as the first 20min after seedling was removed from plasmolyticum and placed back into hypotonic MES buffer. During this period cytoplasm just recovers to fill the entire space outlined by the cell wall, but the cell is still busy working on regaining turgor. Tubules were shorter and thicker and seemed to have less space between each other, which can be analyzed with mesh size calculations in future studies. Plasmolysis was usually seen after 30 min of plasmolyticum addition.

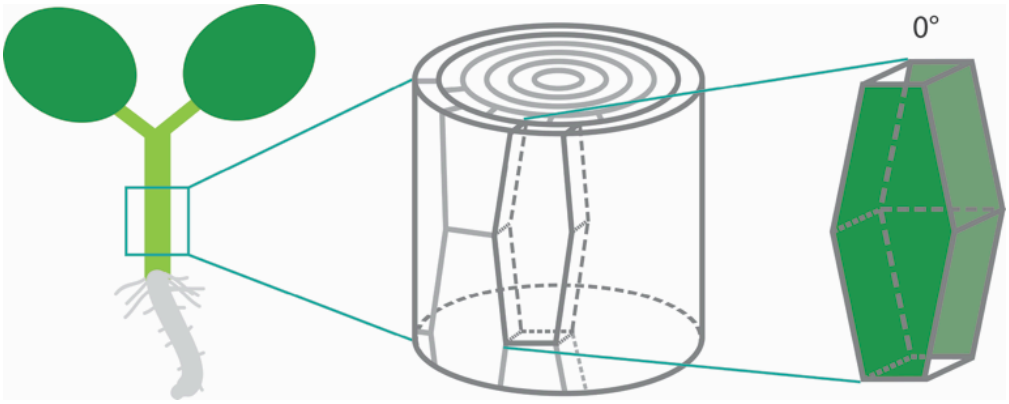

Figure 2-1. Illustration of the orientation of the hypocotyl epidermal cell used to generate 3D reconstruction. The face-on view toward the apical sidewall of the epidermal cell is described as 0°.

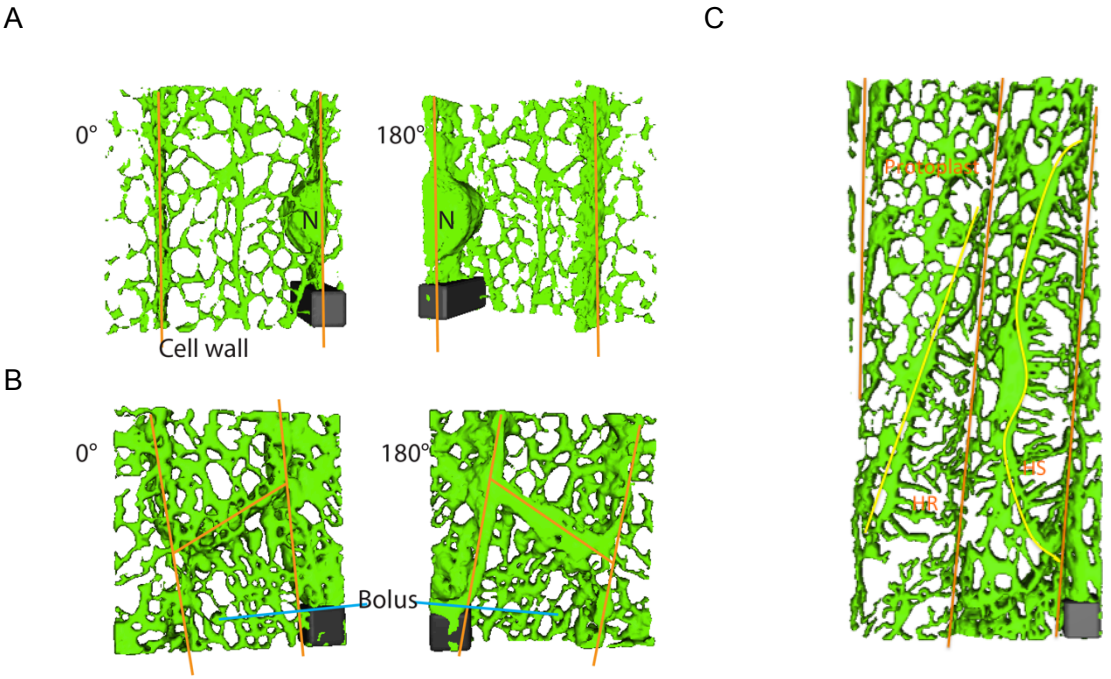

Figure 2-2. ER shape change during plasmolysis in *Nicotiana benthamiana* hypocotyl cells with ER lumen labeled with GFP. N = nucleus. A) 3D reconstruction of ER in control cells. Orange lines indicate cell wall. Bar = 6μm*6μm*15μm. B) 3D reconstruction of ER during the recovery after plasmolysis. Bar = 6μm*6μm*6μm. C) 3D reconstruction of ER during plasmolysis. Yellow line indicates the boarder of protoplasts. Within periplasmic region Hechtian strands (HS) and Hechtian reticulum (HR) can be seen. Bar = 6μm*6μm*5.7μm.

2. Hechtian strands and Hechtian reticulum form within the periplasmic region

As hypothesized by Oparka et al (1994) (*37*), based on ultrastructural analysis and $DiOC_6$ staining, ER is present in Hechtian strands, which have a concentric tubule structure with ER as the center and plasma membrane as the outer tubule. We confirmed this by using *Nicotiana benthamiana* with ER lumen labeled with GFP in fluorescent live imaging. Hechtian strands and reticulum showed continuous green fluorescent labeling extended from the bulk of ER within protoplasts. (Figure 2-2 C and 2-3). Interestingly, 3D-reconstruction shows the Hechtian strands and Hechtian reticulum have not only different branching patterns, but also different spatial

arrangements within the periplasmic region. In earlier studies, Hechtian reticulum appears to be tightly associated with the cell wall while Hechtian strands seems to be linked between protoplast and the Hechtian reticulum in *T. virginiana* leaf epidermal cells (*51*). The arrangements are confirmed by 3D analysis.

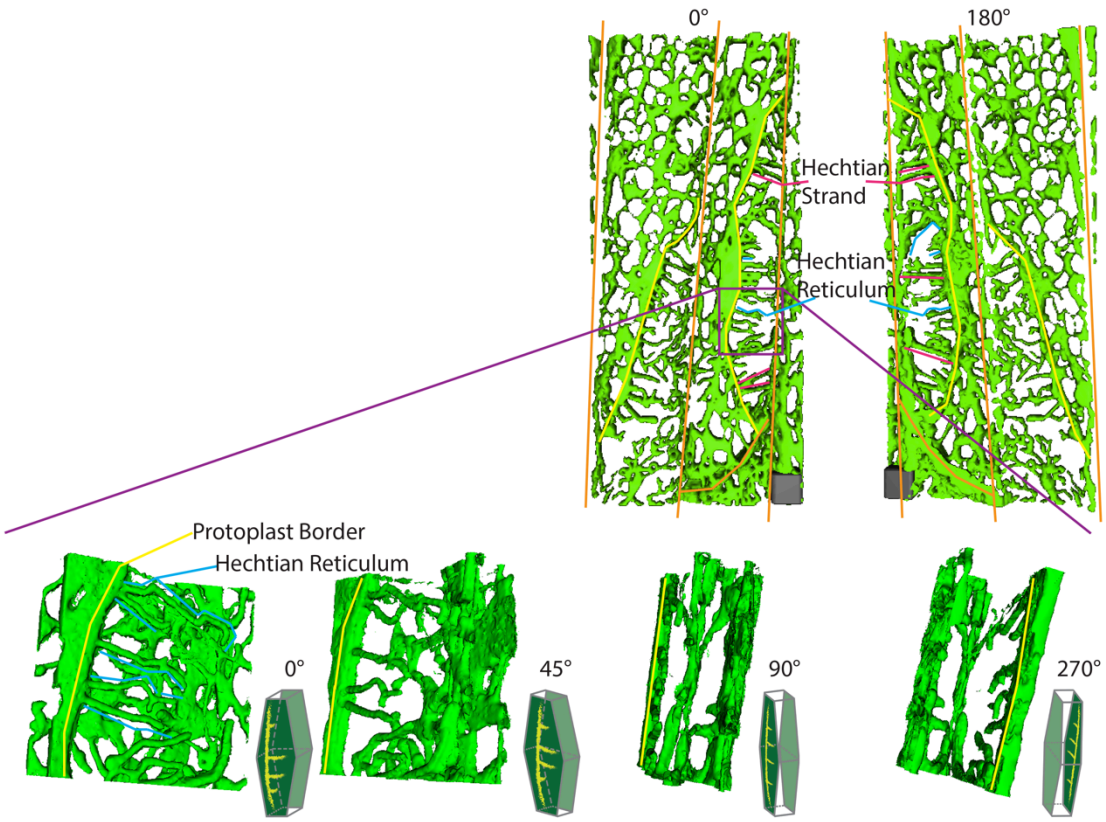

Figure 2-3. 3D reconstructions of ER during plasmolysis. Yellow lines indicate the borader of withdrawing protoplasts. Representations of Hechtian strands and Hechtian reticulum are indicated by magenta and blue lines respectively. Bar = 6μm*6μm*5.7μm. Purple rectangle indicates a specific region where Hechtian strands and reticulum form, with the 3D reconstructions of ER in that specific periplasmic region at the bottom panel. Small inset of each frame indicate the angle of view toward the apical surface of the hypocotyl cell sidewalls.

The organization of ER-containing Hechtian reticulum and strands can be more clearly distinguished using 3D reconstructions. During plasmolysis, both Hechtian strands and Hechtian reticulum are continuous with the ER present in the withdrawing protoplasts (Figure 2-3). Hechtian reticulum, which has a more curved and branched tubular shape, resides in the vicinity of the inner side of the cortical cell wall, anchored either to the cell wall or some other scaffold structure (i.e. cytoskeleton, especially microtubule, discussed later) which keeps the structure stable. Meanwhile Hechtian strands reside deeper in the periplasm, forming a straight, bridge-like link between the protoplast and the cell wall (Figure 2-3).

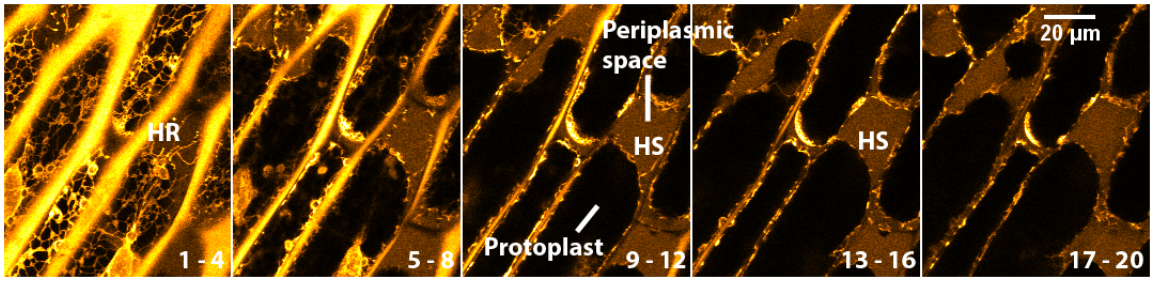

Figure 2-4. Hechtian strands and reticulum locate differently in periplasmic region. Seedlings expressing GFP-HDEL were treated for 45 min with 0.75M sorbitol then incubated in sorbitol + 2.5mg/mL lucifer yellow. Each frame in the montage is the z-projection (Sum slides in imageJ z-project) of 4 adjacent focal planes. Step size of the z-stack is 0.53 µm, so each of the images in the montage is the z-project of a 2.12 µm thick volume in the cell. Slice number indicated at bottom right of each frame. HS = Hechtian strands and HR = Hechtian reticulum respectively. Images are pseudo-colored with LUT = Orange hot in imageJ. Scale bar = 10 µm. Periplasmic spaces are indicated by the relatively low-intensity yellow regions outside the protoplasts.

During plasmolysis, the total volume of the protoplast becomes smaller, as revealed by the filling of the periplasmic space with the wall-permeant fluorescent probe, lucifer yellow. A Z-stack image series was taken from the peripheral to the center of the hypocotyl cell, and every 4 slices (0.53 µm per slice) were stacked (added) together (Figure 2-4, left to right with left corresponding to the cortical region and right to the center of the cell). The regions where protoplasts have withdrawn away from the wall have diffuse fluorescence from Lucifer yellow are periplasmic. An altered network of GFP-HDEL-labeled ER tubules is adjacent to the cell wall (Figure 2-4, sections 1-4, within the first 2.12 µm from the cortical region) and corresponds to the Hechtian reticulum (HR). As the cell is more deeply optically sectioned, tubules marked by the GFP-HDEL ER label occur in the periplasmic space and correspond to the Hechtian strands (HS, Figure 2-4, sections 9-12 and 13-16, 4.24 µm to 8.48 µm from the cortical surface). This result further confirms the organization difference between Hechtian strands and reticulum.

A

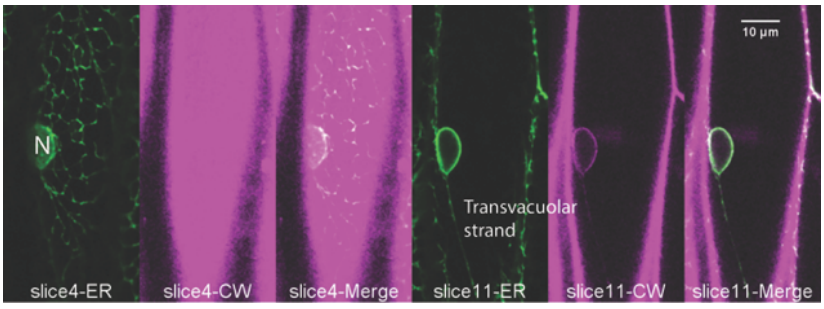

Figure 2-5. Confocal images of ER (green) and propidium iodide (PI, magenta) labeled cell wall at different focal planes. A. ER and cell wall in a control cell. Left 3 images show the focal plane at the cortical ER region. Right 3 images show a focal plane in the middle section of that cell, where ER transvacuolar strands can be seen. B. ER and cell wall in a plasmolyzed cell. Right 3 images show a focal plane in the middle section of the same cell. N = nucleus.

B

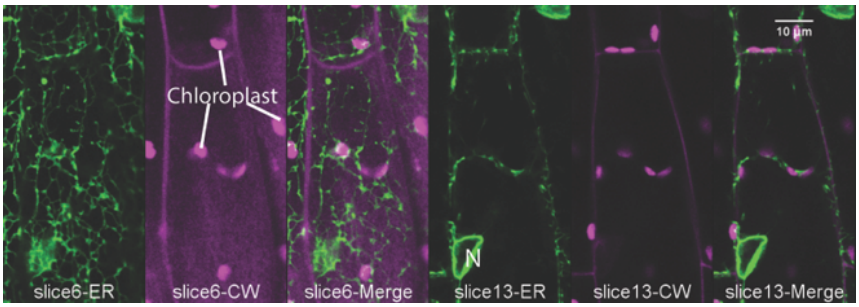

Figure 2-5 Continued.

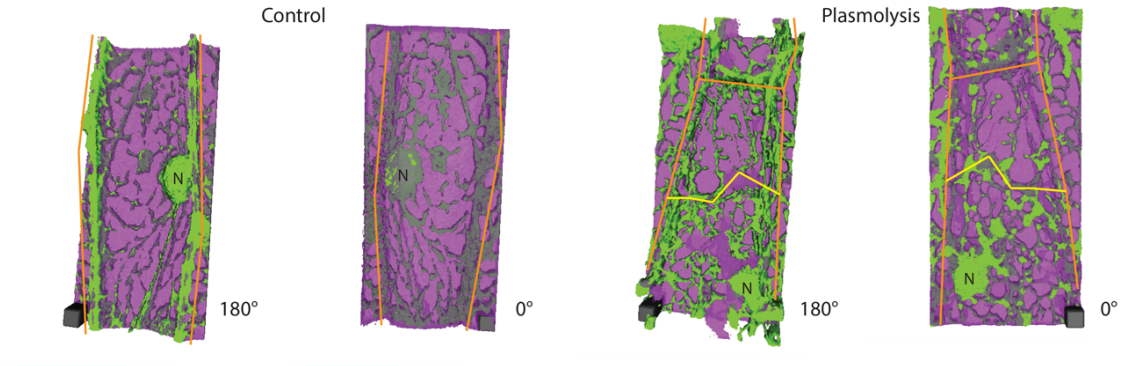

Figure 2-6. 2 channel 3D reconstructions of ER (green) and cell wall (magenta) in control (left 2 images) and plasmolyzed cells (right 2 images). Scale bar 4µm*4µm*10.6µm for control, 4µm*4µm*14.31µm for plasmolysis.

2-channel 3D reconstruction of the GFP-HDEL ER label and propidium iodide cell wall label also supports the results above. In Figure 2-5 and 2-6, the relationships between the cortical ER, Hechtian reticulum and cell wall are shown. In a normal *N. benthamiana*

hypocotyl cell, the cortical ER network is in very close proximity to the cell wall (within 500 nm, the axial resolution limit of the confocal microscope, Figure 2-5 A and 2-6). The ER networks, altered in form and becoming the Hechtian reticulum, remain in the close proximity in plasmolyzed cells, after protoplast pulls away (Figure 2-5 B and 2-6). Note that from 0° view (face-on view) (last panel of figure 2-6) part of the ER (green) appeared to be outside of the cell wall, this is caused by the strong ER signal occuring within the same 500 nm optical section at the same time with the relatively weak cell wall signal. This is because when focal plane approaches cell wall the out-of-focus light from ER is strong enough to show up in the plane where only cell wall localizes.

3. Plasma membrane behavior within the periplasmic region

The formation of the Hechtian strands and Hechtian reticulum occurs in regions of both concave plasmolysis (Figure 2-7 A) and convex plasmolysis (Figures 2-7 B). Convex plasmolysis, where the protoplast forms a convex structure, often forms at the cell's apex, while concave plasmolysis often occurs along the side of the cell. In an effort to see the plasma membrane covering the ER tubules in Hechtian strands and reticulum, cells were labeled with the plasma membrane and endosome dye, FM4-64 and analyzed by 2-channel 3D reconstruction. Note that the FM4-64 label is relatively weak compared to the ER label, and the optical section captures the PM, it also captures some out-of-focus light from the ER in Figure 2-7.

Surprisingly, plasma membrane was shown to cover the entire cortical surface of the epidermal cell in *N. benthamiana* hypocotyl regardless of the fact that protoplast is withdrawing beneath it (Figure 2-7). While at the border of the withdrawing protoplast, plasma membrane still forms a dome that covers the anticlinal facet of the protoplast. This is observed in both concave (Figure 2-7 A) and convex (Figure 2-7 B) plasmolysis, indicating that plasma membrane still withdraws from the anticlinal and distal cell wall. Limited by the resolution of confocal fluorescent microscopy, we cannot resolve the detailed position difference between the ER and plasma membrane, but the 3D reconstruction results indicate that plasma membrane may be folding in underneath the Hechtian reticulum, forming a thin plasma membrane – enclosed chamber holding the ER inside in close proximity to the cortical cell wall.

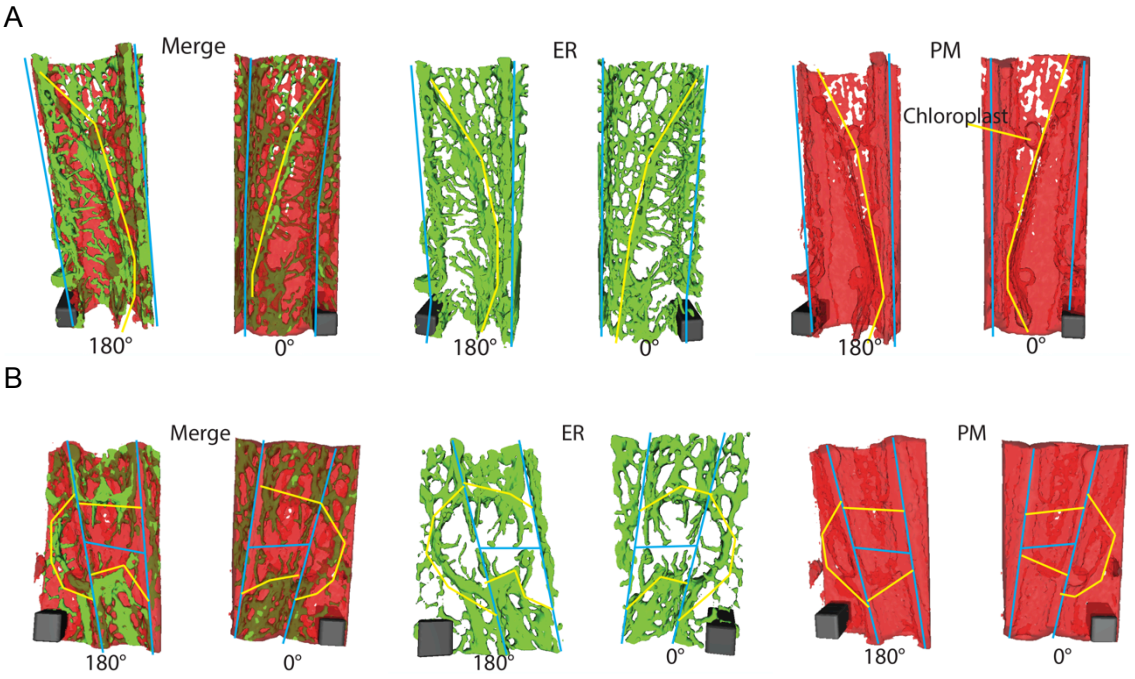

Figure 2-7. 3D ER reconstructions in relation to the position of plasma membrane (PM) in *N. benthamiana* hypocotyl cells with ER lumen labeled with GFP. A) 2-channel 3D reconstructions of ER (green) and plasma membrane labeled with 20 μM/L FM4-64 (red). Bar = 6μm*6μm*15.3μm. Concave plasmolysis is shown. B) 2-channel 3D reconstructions of ER (green) and plasma membrane (red) showing convex plasmolysis. Bar = 6μm*6μm*12μm. Yellow lines indicate the withdrawing protoplast border, blue lines indicate cell wall border.

4. Cytoskeletal association behavior of ER during plasmolysis

As described in Lang-Pauluzzi et al 2000, microtubules were present in Hechtian reticulum. The shape of microtubule shown in periplasmic region was a reminiscent of the ER fluorescence that we have seen in Hechtian reticulum. To study if the ER has any spatial interactions with the microtubule cytoskeleton during the formation of Hechtian strands and reticulum, we created *Arabidopsis* lines with ER-microtubule double labeling. The double-labeled lines were plasmolyzed and confocal Z-stack images were taken in both fluorescent channels for 3D reconstructions. 3D reconstruction of the two channels shows that the ER and microtubule labels co-localize

in Hechtian reticulum (Figure 2-8). The ER strands seem to be tracking on microtubules, since at the end of each branches of the Hechtian reticulum, microtubules are seen without the ER. Note that, depending on the fluorescent signal strength, in some branches the ER appears to be covering microtubule that is co-localized with it. But if we look into the original confocal images in Figure 2-8 A, we can confirm the presence of continuous microtubule strand within that region.

According to the 3D reconstructions shown in Figure 2-8, microtubules co-localize with ER in the Hechtian reticulum and at the same time, they have a more curved form with more branches (Figure 2-9 A right panel) that is different from normally polymerized microtubules (Figure 2-9 A left panel). Meanwhile within the protoplast, polymerized microtubules shift into a more horizontal orientation as described in earlier work (*39*). Within the protoplast a milky background fluorescence is also observed (Figure 2-9 A middle panel), which indicates partial de-polymerization of microtubules within the protoplast. In order to gain insight into the organization and dynamics of these microtubule components (Figure 2-9 A), we photobleached each of them and compared their FRAP profile.

FRAP analysis shows that the recovery half time of polymerized microtubules in control plants has a significantly faster recovery half time when compared to the plasmolyzed protoplast and the Hechtian reticulum (Figure 2-9). However, given that the total extent of recovery is so low due to treadmilling of the microtubules (see below), this is probably due to a low level of diffusing unpolymerized tubulin.

The percent mobility of the control is consistent with polymerized cortical microtubules treadmilling (*52*), producing very low recovery (37.59%) following photobleaching. Microtubule photobleaching recovery is significantly different from control in the Hechtian reticulum where it is the lowest (25.69%). This could either indicate that it is also in polymerized form, but unmoving, or that it is in a non-motile form that is somehow attached to membrane. The fact that the small pool of mobile tubule does recover at a slow rate may indicate a small fraction of moving polymerized tubulin, or a small fraction of tubulin that is moving, but is hindered within the folded-back plasma membrane and ER tubule of the Hechtian reticulum. The highest mobile fraction of

tubulin is in the protoplast (77.29%). This supports our earlier suggestion that the milky background in the protoplast is depolymerized free-diffusive tubulin.

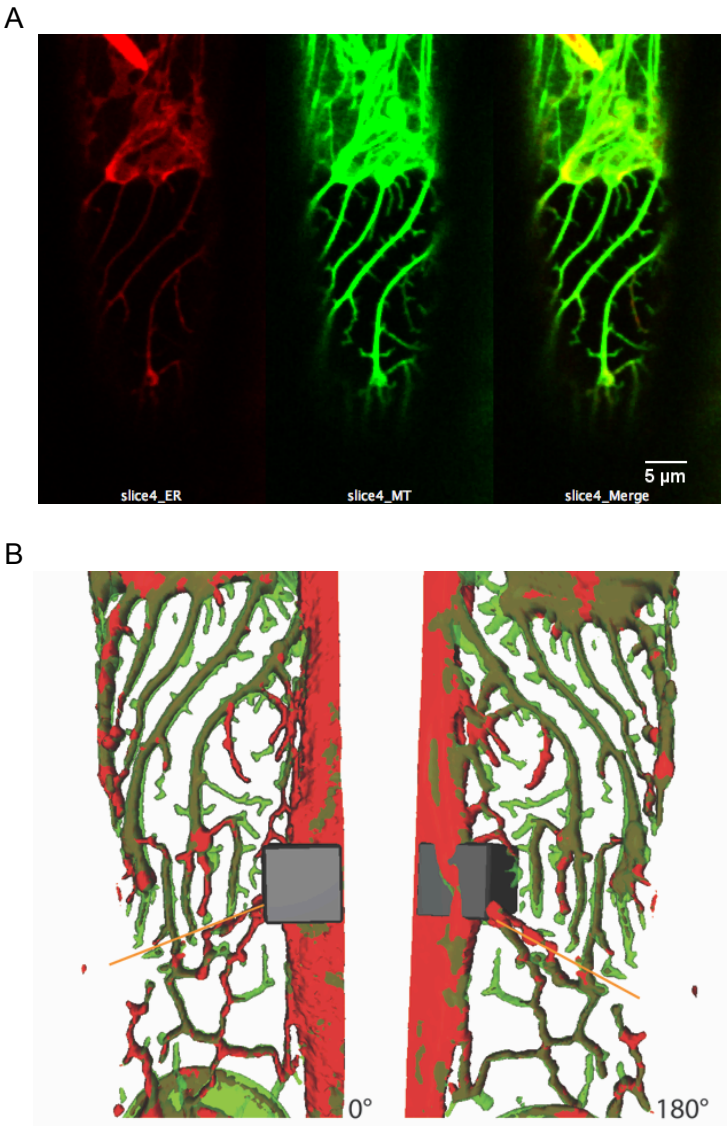

Figure 2-8. Microtubule behavior during plasmolysis in *Arabidopsis* hypocotyl cells with ER lumen labeled by mCherry-HDEL and microtubule labeled by TUA-GFP. A) 2-channel confocal images of a plasmolyzed cell with ER (red) and microtubule (green). B) 2-channel 3D reconstruction of ER and microtubule in Hechtian reticulum to show their co-localization. Transparency of microtubule was adjusted to 50% in order to avoid blocking the thin ER strands that co-localized with it. Bar = 7µm*7µm*10.6µm.

A

B

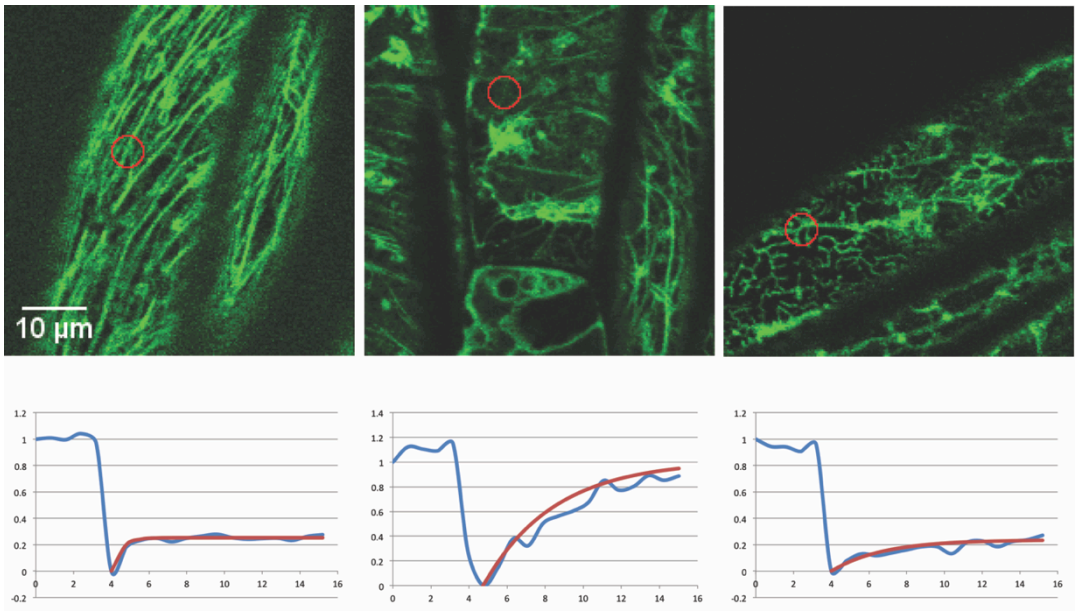

Figure 2-9. FRAP analysis of microtubule at different stages of plasmolysis in *Arabidopsis thaliana*. A) Representative regions of microtubules studies in FRAP analysis. Orange circle indicate photo-bleached area. B) Representative region FRAP normalized intensity (blue) and single exponential fitted recovery curve (red) of the three regions corresponding to A.

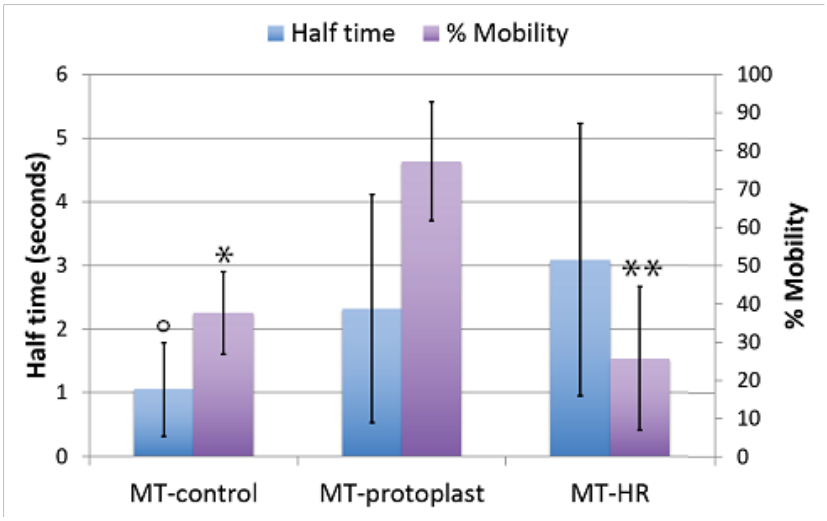

Figure 2-10. FRAP analysis of microtubule at different stages of plasmolysis. Three different types of microtubule components are shown in horizontal axis: normal microtubule strands in control cells, depolymerized microtubule in protoplast during plasmolysis and microtubule presented in Hechtian reticulum. Primary vertical axis (left) shows recovery half time, numbers of circles above the bars indicate significantly different groups ($p<0.05$), N = 38, 49, 55 respectively. Secondary vertical axis (right) shows the percent mobility, numbers of asterisks above the bars indicate significantly different groups ($p<0.05$), N = 38, 49. 57 respectively. Bars: averages. Error bars: standard deviation.

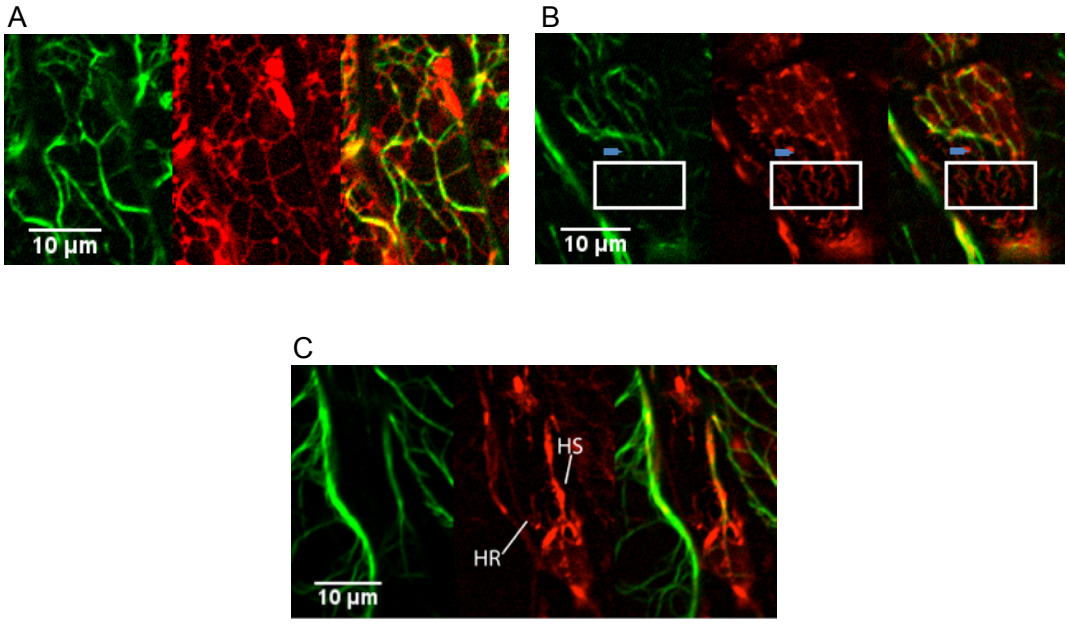

Figure 2-11. ER and actin filaments interaction during plasmolysis in *Arabidopsis thaliana*. 2-channel confocal images of *Arabidopsis* hypocotyl cells with ER labeled by mCherry-HDEL (red) and actin filaments labeled with YFP-ABD2 (green). A) ER tracks on actin within the protoplast during plasmolysis. B) Actin doesn't show up in the majority part of the Hechtian reticulum (white squares) but shows up in a few bigger strands (blue arrows). C) Actin forms a big strand within the periplasmic region but is excluded in the fine network of Hechtian reticulum.

As described in Lang-Pauluzzi et al. (*39*) and Lang et al. (*35*), both actin microfilaments and microtubules were present in the Hechtian strands, but the appearance of actin in the Hechtian reticulum is more obscure. Figure 2-11 A shows that ER remained tracking on actin cytoskeleton in the protoplast, just as in normal plant cells (*16*). In Figure 2-11 C, bundles of actin filaments extended from the protoplast, which corresponds with the shape and position of Hechtian strands. However, there is very limited presence of discernable actin filaments in the vicinity of cortical cell wall where Hechtian reticulum localizes (Figure 2-11 B and C). This is in contrast with the presence of microtubules in

the Hechtian reticulum, as seen in plasmolyzed cells that are dual-labeled with mCherry-HDEL and GFP-TUA6 (Figure 2-8).

Discussion

Our data with seedlings that have ER lumen labeled with GFP and plasma membrane labeled with FM-464 dye show that the region where Hechtian reticulum formed is covered by plasma membrane. Although in our living samples the detailed relationship between the plasma membrane and ER strands within that area is not resolved, this can still be resolved with ultrastructural analysis, e.g., FIB-SEM (*53, 54*). The fact that protoplast is pulling away from the anticlinal and distal facets of the cell leaving a thin layer of cytoplasmic components attaching to the inner surface of the cortical cell wall is quite intriguing. The places where Hechtian reticulum forms may be the potential ER-PM-CW 3-way anchor sites. These anchor sites may play important roles in ER shape and dynamic controls that are also discussed later in Chapter III. Researchers that reported cells lacking Hechtian reticulum formation either through RGD peptide treatment or mutations in NDR1 proteins (*55, 56*) suggested potential candidates for identifying these 3-way anchor sites. These anchor points seems to be only present on the outer and inner periclinal cell walls of the epidermal cell on the hypocotyl, as it is shown in Figure 2-12 A and B. This organization may indicate important orientation information on the polarity of epidermal cells in higher plants. The formation of Hechtian reticulum covered by an intact sheet of plasma membrane indicated no dissociation of the cytoplasmic component and the cell wall. In contrast, on the anticlinal and distal walls anchor points of Hechtian strands appear after protoplast pulls away, some but not all of them were identified as plasmodesmata (*37*). Plasmodesmata are known for connection between plant cells, thus spreading of macromolecules and infection from cell to cell is made possible through them (*57, 58*). If plasmodesmata are only formed on the wall where protoplasts withdraw, this might indicate a special plant supracellular organization where by the outer and inner periclinal wall limit the spread of pathogens such as viruses.

The co-localization of the ER and cytoskeleton in the periplasmic region may suggest the mechanism of how ER tracking along microtubule and actin cytoskeleton

differentially. According to our results Hechtian reticulum ER is exclusively co-localized with microtubule while within the protoplast they still maintained their association with actin. Since plasmolysis is a reversible process, in this case it can serve as a tool to isolate the portion of ER which only tracks on microtubules. In future studies, altering Hechtian reticulum microtubules by oryzalin treatment may reveal mechanisms for ER tracking on microtubules. Hechtian-reticulum microtubules show a different FRAP pattern compared to polymerized microtubule FRAP, which indicates a different organization of microtubules. If the depolymerization agent oryzalin promotes a diffusive FRAP pattern in Hechtian reticulum microtubules, then it is likely that Hechtian reticulum microtubules are organized in a novel polymerized state. This state can be confirmed with electron microscopy. The potential mechanism for the formation of this specific form of microtubule is likely to involve association with the plasma membrane.

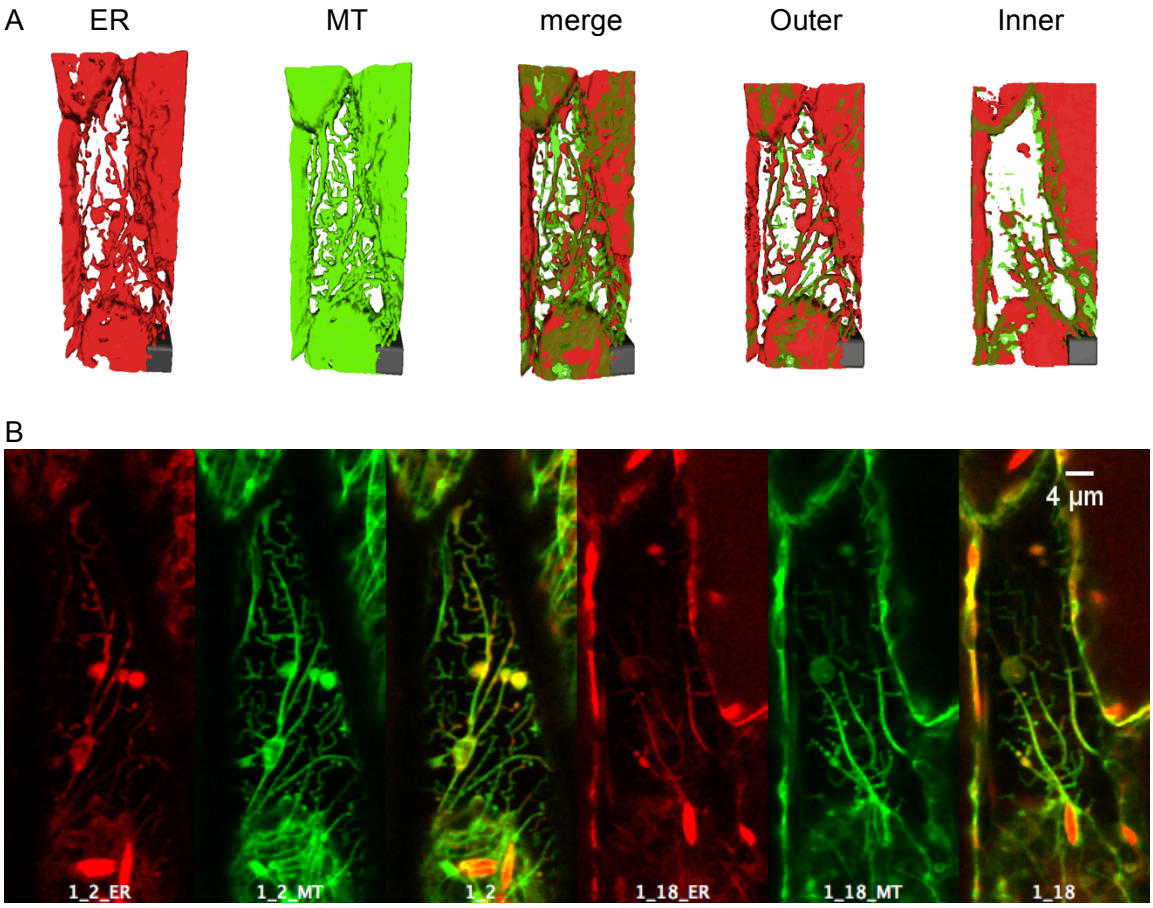

Figure 2-12. Microtubule and ER behavior during plasmolysis in *Arabidopsis thaliana* hypocotyl cells with ER lumen labeled by mCherry-HDEL and microtubules labeled by GFP-TUA6. A) 3D reconstruction of ER and microtubule in different focal planes. Left 3 panels are the whole cell reconstructions, 4th panel is the outer periclinal section of the same epidermal cell, 5th panel is the inner periclinal section of the same epidermal cell. B) Confocal images of the same cell used in A at different focal planes.

CHAPTER III

PLASMOLYSIS ER DYNAMICS AND ITS INFLUENCE ON CYTOPLASMIC STREAMING

Introduction

Although the basic structural components are present in most cell types in eukaryotes, the organization of the ER differs depending on the cell type and its stage of development. ER morphology and dynamics change not only with development (for example as cells elongate), but also under abiotic and biotic stress (*8*). Previous studies in our lab on ER morphology under osmotic stress indicate that in *N. benthamiana* hypocotyl cells, ER becomes more cisternalized after seedlings are exposed to hyperosmotic solutions (Figure 1-1 B and D) (*17*). Studies on ER morphology in shorter, meristematic cells and fully elongated cells in *Arabidopsis* root showed that in more elongated cells the ER is more tubular (Figure 1-1 C and E) (*18*). Interestingly, as the protoplast shrinks in size, the cisternalized ER (Figure 1-1 D) phenotype is a reminiscent of ER in shorter cotyledon cells (Figure 1-1 C) (*18, 59*). This raises the question of whether the ER senses the length of the cell (or protoplast in the case of plasmolysis). Becasue plasmolysis is a reversible physiological event, it becomes a valuable tool for us to manipulate the protoplast size, as well as the organization of ER and to study the changes of ER shape. A change of maximal ER streaming rate accompanies its shape change as the cell elongates. Using Kbi optic – flow analysis, researchers were able to identify the difference in ER streaming rate in “fast lanes” at different stages of plant development. In 3-day-old *Arabidopsis* cotyledon cells, ER streaming rate is significantly lower (0.5 μm/s) than that of 12 day old seedlings (1.5 μm/s) (*59*). Similar types of decrease in ER dynamics may occur correspondingly as the ER becomes more cisternalized in shrunken protoplasts. But again, Kbi optic – flow analysis based on tracking the GFP movement within the ER lumen did not separate translational movement, ER remodeling and the luminal flow of ER proteins. Also, those analyses were done within the part of ER network known as “fast lanes”, where rates of remodeling are remarkably higher than that from the “slow lanes”. To study whether the

remodeling of ER tubules and cisternae changes as the protoplast shrinks in size, morphological image processing was used to determine the size of the tubules and cisternae and persistency mapping was used to quantify the persistency of these two types of ER elements. Using a persistency mapping macro in ImageJ, we are able to separate the displacement or translation events in the remodeling of the ER from the flow that occurs within the tubules and cisternae (*11, 12*). While persistency mapping gives us the persistency of either tubules or cisternae, a pixel-based optic flow analysis allows us to measure the total movement of ER. The relative movement of ER will be calculated by dividing the area of the total moving parts of ER by the total membrane area. Our pixel-based optic flow analysis only analyzes the total movement of the entire ER network. Within the total movement, the component of luminal flow is, however, expected to be low because the ER lumen marked with GFP is homogenously fluorescent. Thus our method mainly stands for the movement created by ER remodeling and translation.

ER was speculated as one of the potential driving forces of cytoplasmic streaming (*60*). If the movement of ER goes down during plasmolysis, we expect to see the streaming of other membranebound organelles to decrease correspondingly. Lipid bodies are minute membrane-bound organelles that range in size from about 0.5 to 2.5 μm, and which are pinched off from the endoplasmic reticulum (*61*). Lipid bodies can be identified in DIC images by their diameter, circular shape, and high level of refraction. Here we use lipid bodies as an indicator of cytoplasmic streaming to study whether cytoplasmic streaming changes corresponding to changes in ER shape and dynamics during plasmolysis.

Materials and methods

Time-lapse images for persistency mapping were acquired using an Olympus FV1000 confocal microscope with a 1.2NA UPLSAPO water immersion 60X objective. Argon ion laser line with excitation wavelength 488 nm was used to excite GFP-labeled ER lumen, emission was set to 510 nm. A 70-frame time-lapse movie with frame interval 0.32s is acquired for each cell-of-interests, and the first 50 frames of it are used for persistency mapping. Seedlings were kept stable during the period of time-lapse image recording to

eliminate frame shift. Persistency mapping was carried out using a home-developed macro in imageJ, as described in Sparkes et al 2009 (*12*).

The related movement of ER is calculated by dividing the integrated density of the total moving parts of ER with the total membrane area. Total moving parts of the ER is calculated by Z-project all the images we got from subtracting each frame of the time-lapse video by the fifth frame after it, and then measure the integrated density of the Z-project image. Total membrane area is calculated by Z-project every frame of the original video, convert it into 8-bit image, threshold between (25, 255), and run Analyze particles with size = 0-Infinity and circularity = 0.00-1.00. The value of total membrane area is the sum of all the particle areas.

Organelle streaming was carried out on the 13th to 40th slides (the portion after finishing bleaching) of the ER luminla GFP FRAP video in *Nicotiana benthamiana* that will be discussed later. A substack of the 13th to 40th slides was first generated, the lipid bodies that moved out of the field of view during the time spam of these 28 slides are excluded, among the rest the two fasted moving lipid bodies was chosen and tracked manually by using Manual Tracking plugin in ImageJ software (*62*). Each instant velocity calculated based on the displacement between two adjacent slides are recorded by the plugin, they are then averaged in Microsoft Excel and the averages were pooled to calculate average and conduct statistical analysis. Statistical analysis was done using student t-test in Microsoft Excel.

Results

1. Protoplast ER become persistently cisternalized during plasmolysis

In an effort to quantify the changes of ER cisternae and tubule area that we have seen in Figure 2-1, persistency mapping was used to isolate and quantify those two parts. At different stages of plasmolysis, persistency maps were generated to calculate the ratio of persistent membrane to the total membrane area (*12*). Both persistent cisternae (Figure 3-1 B) and persistent tubules (Figure 3-1 C) were isolated by thresholding the objects that has the intensity between 0-180 grey level out of the inverted 8-bit

persistency map (0-255, z-projection of a 45-slice binary stack), which equals to the ER component that has been localized persistently in the same spot for 11.2 seconds (35 frames with 0.32 s frame interval) within the time-lapse video.

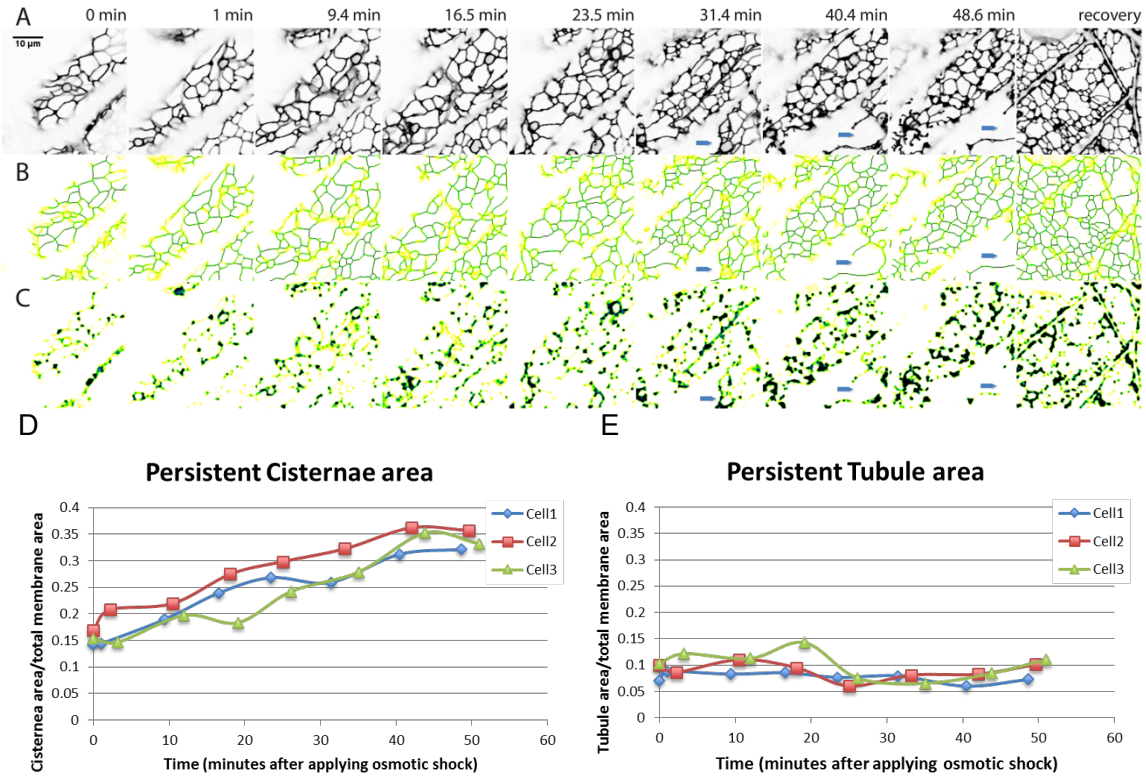

Figure 3-1. Change in amount of persistent ER cisternae and tubules after plasmolysis in *N. benthamiana* seedlings with ER lumen labeled with GFP-HDEL. A - C) Z-projection and persistency map based on confocal fluorescent time-lapse movie taken at different time points. Numbers on each column indicate minutes after starting treatment with 0.75 M sorbitol, the plasmolyticum. Recovery is within 20 min of sorbitol wash-out. Blue arrows indicate where protoplast withdrew from the cell wall. Darker colors indicate more persistent parts of ER. A) Z-projection of the stack inverted to show the general structure of ER in black. B) Persistency map of ER tubule. C) Persistency map of ER cisternae. D) Cisternae persistency in three different representative cells (indicated by different colors and symbols) over the times indicated after treatment with sorbitol, and E) Tubule persistency in the same three cells.

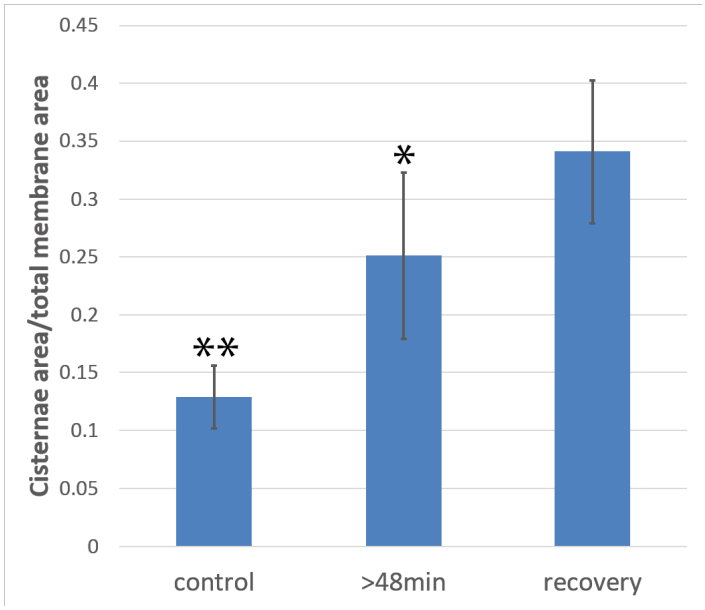

Figure 3-2. Changes in persistent cisternal area over time as percent of total membrane imaged. 3 time points were chosen for comparison: control (before treatment), plasmolysis (after 48 min of treatment) and during recovery. Different numbers of asterisks indicate significant difference with $p<0.05$. Bars: averages. Error bars: standard deviation, N = 10 cells.

Among those persistent structures, individuals with a membrane area >0.3 μm^2 were measured. Persistent cisternae area increased over the time course of the osmotic treatment. As seen in Figure 3-1 C there are growing areas of darker cisternae, and in Figure 3-1 D, the area trendlines are increasing. In contrast, the persistent tubule area remained relatively constant (Figure 3-1 B and E). Significant differences (Figure 3-2) in the area of equally persistent cisternae exist between cells prior to plasmolysis, after plasmolysis (time points taken at after 45 min hyperosmotic treatment) and during the first 20 min of recovery from plasmolysis, i.e., deplasmolyzed cells. The increase in persistent cisternae is probably a combination of both a decrease in the movement (translational and remodeling) of cisternae (Figure 3-3), as well as an increase in the amount of membrane in cisternae.

A

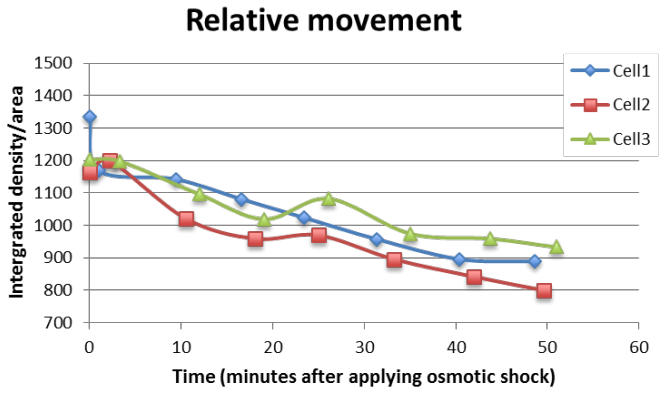

B

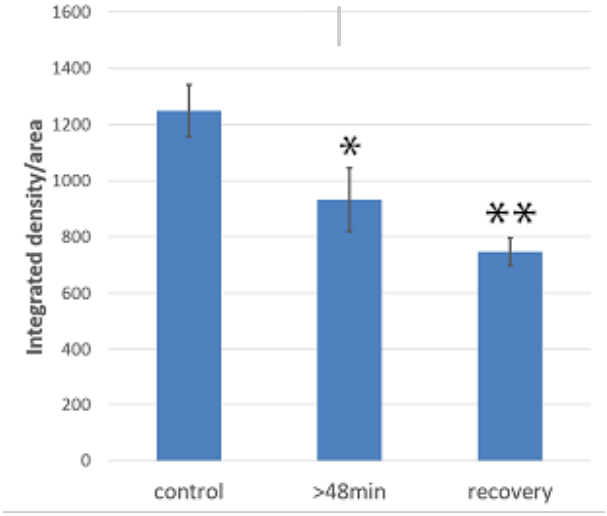

Figure 3-3. Relative movement of ER during plasmolysis in *Nicotiana benthamiana* seedlings with ER lumen labeled with GFP. A) Movement of ER analyzed with pixel-based optic flow in three separate representative cells indicated by different colors and symbols. B) Statistical analysis of movement of ER before and after plasmolysis and during recovery (N = 10). Bars indicate averages and error bars represent standard deviation. Different numbers of asterisks above each group indicate that all of the treatments are significantly different ($p<0.05$).

2. Total movement of protoplast ER diminishes during plasmolysis

The relative movement of the entire protoplast ER membrane is calculated from the difference in pixel intensities that occurs between every five frames (1.6 seconds). Those that moved the most show the highest values and when the integrated intensity of the difference frame is calculated, it provides a pixel-based optic flow measurement of the translational movement of the ER cisternae and tubules. During the plasmolysis, the relative movement of the total protoplast ER diminishes (Figure 3-3 A). There is a significant difference between the amount of relative movement of the ER in control and plasmolyzed cells (48 min after treatment starts) (Figure 3-3 B). This decreased movement corresponds to increased persistent cisternalization (Figure 3-1, 3-2). There is an even further reduction of ER movement in the first 20 min of recovery when plants were transferred back into pH 5.8 MES buffer (Figure 3-3 B), which accompanied higher degrees of cisternalization (Figure 3-1, 3-2).

3. Streaming of lipid bodies slows down is correlated with changes in ER movement and cisternalization

As the protoplast shrinks during plasmolysis, the total ER movement diminishes while the area of persistent cisternae increases. Highly refractile with 1-2 micrometer diameter organelles, putatively the lipid bodies, were observed with differential interference contrast microscopy (DIC) during the time course of plasmolysis experiments. They were used to measure streaming within the cytoplasm. The results show that these organelles also have significantly slower rates of movement upon plasmolysis (Figure 3-4). There is a possibility that this is simply the result of artificially diminishing the cell size and that streaming rates correlate with cell size (*59, 63*). However, within the first 20 min of recovery during de-plasmolysis, when the cell resumes its previous size, the streaming rates remain low (Figure 3-4). This doesn't support the correspondence between cell size and cytoplasmic streaming but it corresponds to the decreased movement rates of the highly cisternalized ER under different conditions (*11, 59*) (Figure 3-3).

A B

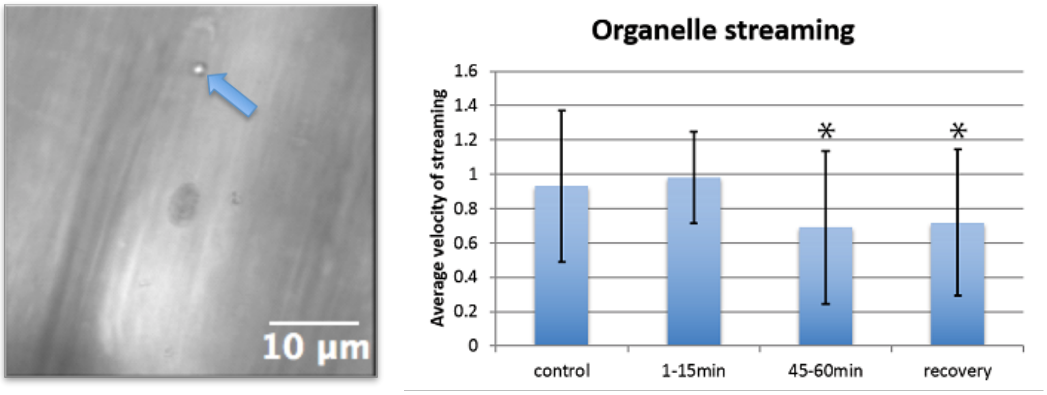

Figure 3-4. Streaming of organelles identified with differential interference contrast microscopy (DIC) in the same cells analyzed for ER luminal flow (Figure 4-1). A) Lipid body identified in DIC images. B) Lipid body streaming rate change at different stages of plasmolysis. Asterisks indicate that after 40 min and during recovery from plasmolysis, organelle streaming is significantly ($p<0.05$) diminished. Bars represent averages and error bars represent standard deviation. N = 40 for each group.

Discussion

Upon plasmolysis and deplasmolysis, there is increased cisternal area and persistency of cisternal ER which is correlated with less movement (cytoplasmic streaming and ER remodeling). This brings up the question of whether the shape of ER influences its mobility and the mobility of other organelles. Interestingly, under other conditions in *Arabidopsis* the same kind of correlation also exists. First, there is a relationship between the functional absence of those myosin motors that drive streaming and increased cisternalization and decreased ER movement (*11*). Second, mutation of ER membrane protein RHD3 also cause the cisternalization of ER, together with more cisternalized ER in younger cotyledon cells, all displayed slower cytoplasmic streaming. A model that is consistent with these observations is that plasmolysis affects the ability of the ER to interact with the actin cytoskeleton and engage in movement via certain

myosins. Analysis of the movement of the ER during normal development, and the involvement of different myosins and other proteins that interact with both the ER and actin, in that movement may allow us to uncover the basic regulators behind this process.

One such process that controls ER remodeling may be the ability of the ER to undergo homotypic fusion. Proteins homologs that mediate ER membrane homotypic fusion have been identified in various different species in recent studies (*29-31*). Among them, ER membrane protein RHD3 has been shown to alter the shape of ER into a more cisternalized state (*59*). Other proteins like Rab10 are identified to facilitate the elongation of new ER tubules (*28*). The remodeling of ER membrane shape may be involved in these processes that modify the organization of the membrane. If the changes in expression level and dynamic behavior of those proteins correspond with the altered ER shapes in the developing cell, new lessons could be learnt in how homotypic fusion mediates the remodeling of ER.

CHAPTER IV

CHANGES IN PROTEIN MOVEMENT WITHIN THE ER LUMEN

Introduction

In earlier studies on ER luminal protein streaming, the translational movement of the ER and the movement of material within the network are not separated, but analyzed together, using an optic – flow method (KBI flow, an ImageJ plugin). These analyses are thresholded to only include the "fast lanes" of ER – regions of the cortical cytoplasm where the ER is not organized in polygons, but as streaming interconnected tubules (*13, 59*). Results of those studies have shown that the ER fast lanes have directional flow. With ER lumen marked with GFP-HDEL, optic flow analysis showed that the fast lane of ER strands have a maximum speed of 1.35 μm/sec in *Arabidopsis* cotyledon petiole cells (*13*). Studies using photoactivable GFP-calnexin trans-membrane domain fusion protein as ER membrane marker also showed evidence for directional flow of ER membrane (*32*). Nevertheless, these studies did not differentiate between the flow of either membrane or luminal ER protein within a relatively stable frame of ER and the translational movement of the ER.

On the other hand, whether the luminal flow or the surface flow of the ER is influenced by the shape of the ER surrounding membrane (tubule or cisternae) and the level of dynamics (constantly remodeling or stable) or not remains a question to be answered. In animal studies, the 3D organization of the ER network has been shown to change the rate of diffusion of ER luminal proteins (*64*). As the ER cisternae becomes bigger and tubules appear to be thicker (Figure 2-2) while the dynamics of ER diminishes during plasmolysis (Figure 3-2, 3-3), and newly formed thin ER tubules appear within Hechtian reticulum and strands, it becomes of interest to see whether the protein flow changes within the ER lumen. Thus in our studies, we will independently assess the luminal flow of ER using Fluorescence Recovery after Photobleaching (FRAP). Photobleaching will be conducted on *N. benthamiana* seedlings with ER labeled with luminal GFP-HDEL. In this case as long as the specific region of ER remains stable within the region of interest (ROI) during the analysis, the recovery of fluorescence only depends on the ability to

move within the lumen, while the lumen itself is contoured by the ER membrane with different shape.

Materials and methods

Photobleaching of ER lumen-GFP was carried out in Olympus FV1000 laser scanning confocal microscope, by using 405 nm diode laser that was set to 100% transmission. A 40-frame (41.4X41.4 μm^2, 200X200 $pixel^2$) video was taken for each bleaching event, with a frame interval 0.32 seconds. Bleach start after recording first 10 frames in a 4.14X4.14 μm^2 (20X20 $pixel^2$ smaller ROI), lasting 368.64 ms. For FRAP analysis, all frames of the videos were acquired as 16-bit gray-scale images. Each analyzed video was first processed with Image stabilizer plugin of ImageJ (*49*). A polygon that selected only the cell being bleached is manually created and added into ROI manager and used for normalization. FRAP analysis was then carried out using FRAP profiler final plugin in ImageJ (*50*). Recovery halftime and percent mobility was collected from each image and used for statistical analysis.

Statistical analyses were carried out by both R and JMP softwares using Tukey-Kramer HSD analysis. One-way ANOVA analysis is also used in JMP to compare multiple groups. Confidence level is at 95% ($p<0.05$) Comparison of FRAP recovery halftime and percent mobility was done between each group of ER components (ER cisternae and tubule in control, plasmolysis and recovery stages respectively, Hechtian strand, Hechtian reticulum during plasmolysis and Bolus during recovery) respectively.

Results: Photobleaching of ER luminal proteins reveals shape related FRAP pattern

Although the measurement of the movement within the ER is sometimes combined with the measurement of the translational movement of the ER when using some types of optic flow analysis (*13, 59*), here we independently assess the movement within the ER lumen using FRAP. In previous studies where both FRAP and photoactivation were used to analyze flow within the ER (*12*), changes in internal flow did not correlate with increased persistency of the ER. Likewise, while plasmolysis increases cisternal

persistency (Figure 3-1, 3-2) and decreases ER translational movement in the protoplast (Figure 3-3), it does not change the half-time of fluorescence recovery or the percent mobility of ER luminal protein in the protoplast (Figure 4-1 C and D). Figure 4-1 A and B shows representative regions and results from FRAP experiments. Note that Hechtian strands and reticula form during plasmolysis, boluses or aggregates of GFP-HDEL only form upon deplasmolysis (Figure 4-1 A, Figure 1-1 B), while cisternae and tubule ER present in all stages. Experimental data from many cells indicate that the half time for recovery does not change in the protoplast during plasmolysis, but increases significantly in Hechtian strands, Hechtian reticulum and boluses (Figure 4-1 C).

Interestingly, although the percent mobility of the GFP-HDEL does not change in the protoplast ER compared to control cells, there are significant decreases in the percent of mobile GFP-HDEL in Hechtian strands, Hechtian reticulum, and boluses (Figure 4-1 D). For a bolus formed within the recovery period, the amount of recovered fluorescence decreased several fold and is significantly lower than that in the rest of the ER. But for Hechtian strands and reticulum, although there is significant decrease in fluorescence recovery, only the ER tubules during plasmolysis and cisternae in control and plasmolyzed cells have significantly higher recovery (Note that Hechtian strands and cisternae during plasmolysis are not significantly different, but the p value is as small as 0.0507, thus Hechtian strands basically differ from the same ER components as Hechtian reticulum).

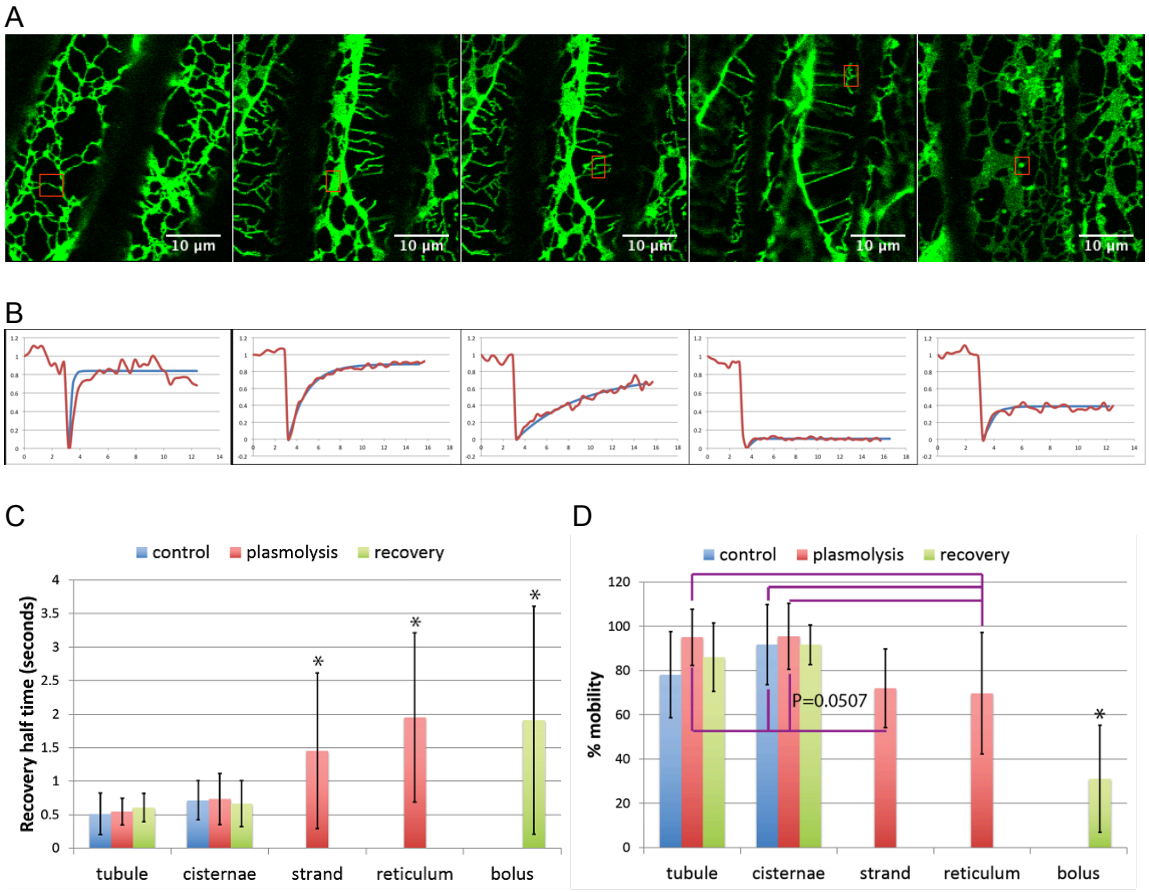

Figure 4-1. FRAP of different regions of the ER lumen GFP before and during plasmolysis and following recovery from plasmolysis in *N. benthamiana* seedlings. A) Images showing representative regions being assessed by FRAP. B) Representative region FRAP normalized intensity (red) and single exponential fitted recovery curve (blue). C) Recovery half-time of GFP-HDEL in tubules, cisternae, Hechtian strands and reticulum, and boluses that form upon deplasmolysis. Numbers of circles above each bar indicate significantly different groups ($p<0.05$). N = 18, 12, 13, 23, 9, 11, 24, 18, 12 for each bar from left to right respectively. Bars: averages. Error bars: standard deviation. D) Percent mobility of the GFP-HDEL in tubules, cisternae, Hechtian strands and reticulum, and boluses that form upon deplasmolysis. Purple lines indicate the pairs of comparison that are significantly different from each other ($p<0.05$). Note that Hechtian strands and cisternae during plasmolysis are not significantly different, but the p value is as small as 0.0507, close to 0.05. N = 18, 12, 13, 23, 9, 11, 24, 18, 13 for each bar from left to right respectively. Bars: averages. Error bars: standard deviation.

Discussion

For the bulk of ER within protoplast, plasmolysis increases its cisternal persistency (Figure 3-1, 3-2) and decreases ER translational movement. The most obvious shape change would be the enlargement of ER cisternae. Recent biophysical studies on the influence of 3D ER shape on ER luminal and surface protein diffusive flow indicate that organelle shape considerably influences diffusive transport (*64*). Studies on ER membrane shaping protein reticulons also showed that reticulons restricted narrow ER tubules can have limited luminal protein flow (*21*). The fact that protoplast ER doesn't have obvious changes in FRAP profile indicate that the shape of ER membrane caused by plasmolysis wasn't enough to induce changes in luminal protein flow.

The highly tubulized ER in Hechtian strands and reticulum indicate a potential lack of space for ER lumen protein to move around freely. But if the tubular shape of Hechtian strands and reticulum do not restrict the flow within their lumen, the reduction of both speed and amount of fluorescence can be inferred as the result of being isolated from the bulk of ER within the protoplast. The percent mobility for Hechtian strands and reticulum are diminished but are still about 70% of pre-bleaching value, thus the flow is not likely to be physically blocked. The streaming within the protoplast was reduced but not eliminated (Figure 3-4), thus indicating that directional flow within the protoplast is still going on. The phenomenon that fluorescence within the Hechtian strands and reticulum can still recover but recovers slowly may be caused by the lack of directional flow outside the protoplast. In FRAP analysis, whether there is asymmetry in recovery pattern in protoplast ER lumen or not could be used to determine the direction of flow within the ER lumen. Boluses were speculated as "broken pieces" from Hechtian strands and reticulum that could not fuse back to protoplast ER at the early stage of recovery, which explains their lack of fluorescence recovery.

CHAPTER V

SUMMARY

ER, as the largest endomembrane system in eukaryotes, plays important roles in protein and lipid synthesis and distribution (*8*). Our studies of ER dynamics provide evidence for an underlying function of this network organization in connecting organelles with a “highway” of protein and lipid flow (*65*). The well-maintained complicated ER network addresses many important functions inside the cell. For example, it could be important for providing the generation force behind bulk flow cytoplasmic streaming in the mature higher plant cell, as it has been suggested for giant algal cells (*60*). The contact sites of ER and other organelles, such as mitochondria, may have critical functions in creating communication and routes of metabolites exchange between organelles (*9*). Either flow within the cytoplasm or new ways for metabolites exchanges is important for plant development. Study the relationship between ER morphology and these processes helps us to understand the basic mechanism of cell growth. In particular, the response of the ER to biotic, and as detailed here, abiotic stress, could play a role in overcoming or evolving with that stress.

Hechtian strands and Hechtian reticulum forms at where ER is not able to pull away from cell wall. Our results showed that Hechtian reticulum specifically localizes right beneath the periclinal wall. More interestingly, the layer where Hechtian reticulum forms is covered by plasma membrane, which normally is considered withdrawn away with the receding protoplast. Thus using plasmolysis as a tool, we are able to identify potential ER – plasma membrane – wall anchoring sites, which might have an important role in shaping the cortical ER network. These plasma membrane contact sites in animal cells and yeast have been identified as the sites of cholesterol transport and lipid biosynthesis (*66*). The initiation of new contact sites and the associated reorganization of the ER is also a key process in the initial stages of the entry of symbiotic nitrogen-fixing bacteria, the initial association of mycorrhizal fungi with roots, and the intiation and development of tip growth (*8*). Pathogen defense studies identified a plasma membrane-localized protein NDR1 mutant that cannot form Hechtian reticulum and have impaired pathogen defense signaling (*56*). Our results gave detailed descriptions

of the Hechtian reticulum formation, its relationship to the rest of the cell and cytoskeletal interactions, which would be important in identifying ER function in pathogen defense signaling. Future studies using mutants with defective proteins involved in Hechtian reticulum formation will be carried out to examine the roles of these proteins in ER shaping and material transport. Study of the membrane contact sites, the Hechtian reticulum and Hechtian strand attachment regions, could provide insight into the basic function of this association in multiple physiological events, from nutrition to growth to pathogen defense in the life of plants.

REFERENCES

1. B. Alberts, *Molecular Biology of The Cell*. (Garland Science, ed. 5, 2014).

2. A. R. English, G. K. Voeltz, Endoplasmic reticulum structure and interconnections with other organelles. *Cold Spring Harb Perspect Biol* **5**, a013227 (2013); published online EpubApr (10.1101/cshperspect.a013227).

3. M. Puhka, M. Joensuu, H. Vihinen, I. Belevich, E. Jokitalo, Progressive sheet-to-tubule transformation is a general mechanism for endoplasmic reticulum partitioning in dividing mammalian cells. *Mol Biol Cell* **23**, 2424-2432 (2012); published online EpubJul (10.1091/mbc.E10-12-0950).

4. Y. Shibata, G. K. Voeltz, T. A. Rapoport, Rough sheets and smooth tubules. *Cell* **126**, 435-439 (2006); published online EpubAug 11 (10.1016/j.cell.2006.07.019).

5. P. Wang, T. J. Hawkins, C. Richardson, I. Cummins, M. J. Deeks, I. Sparkes, C. Hawes, P. J. Hussey, The plant cytoskeleton, NET3C, and VAP27 mediate the link between the plasma membrane and endoplasmic reticulum. *Curr Biol* **24**, 1397-1405 (2014); published online EpubJun 16 (10.1016/j.cub.2014.05.003).

6. A. G. Manford, C. J. Stefan, H. L. Yuan, J. A. Macgurn, S. D. Emr, ER-to-plasma membrane tethering proteins regulate cell signaling and ER morphology. *Dev Cell* **23**, 1129-1140 (2012); published online EpubDec 11 (10.1016/j.devcel.2012.11.004).

7. P. K. Hepler, B. A. Palevitz, S. A. Lancelle, M.M. McCauley, I. Lichtscheidl, Cortical endoplasmic reticulum in plants. *J. Cell Sci.* **96**, 355-373 (1990).

8. L. R. Griffing, C. Lin, C. Perico, R. R. White, I. Sparkes, Plant ER geometry and dynamics: biophysical and cytoskeletal control during growth and biotic response. *Protoplasma*, (2016); published online EpubFeb 10 (10.1007/s00709-016-0945-3).

9. B. Kornmann, E. Currie, S. R. Collins, M. Schuldiner, J. Nunnari, J. S. Weissman, P. Walter, An ER-mitochondria tethering complex revealed by a synthetic biology screen. *Science* **325**, 477-481 (2009); published online EpubJul 24 (10.1126/science.1175088).

10. L. R. Griffing, Laser stimulation of the chloroplast/endoplasmic reticulum nexus in *tobacco* transiently produces protein aggregates (boluses) within the endoplasmic reticulum and stimulates local ER remodeling. *Mol Plant* **4**, 886-895 (2011); published online EpubSep (10.1093/mp/ssr072).

11. L. R. Griffing, H. T. Gao, I. Sparkes, ER network dynamics are differentially controlled by myosins XI-K, XI-C, XI-E, XI-I, XI-1, and XI-2. *Front Plant Sci* **5**, 218 (2014); published online EpubMay (10.3389/fpls.2014.00218).

12. I. Sparkes, J. Runions, C. Hawes, L. Griffing, Movement and remodeling of the endoplasmic reticulum in nondividing cells of *tobacco* leaves. *Plant Cell* **21**, 3937-3949 (2009); published online EpubDec (10.1105/tpc.109.072249).

13. H. Ueda, E. Yokota, N. Kutsuna, T. Shimada, K. Tamura, T. Shimmen, S. Hasezawa, V. V. Dolja, I. Hara-Nishimura, Myosin-dependent endoplasmic reticulum motility and F-actin organization in plant cells. *Proc Natl Acad Sci USA* **107**, 6894-6899 (2010); published online EpubApr 13 (10.1073/pnas.0911482107).

14. C. Hawes, P. Kiviniemi, V. Kriechbaumer, The endoplasmic reticulum: A dynamic and well-connected organelle. *Journal of Integrative Plant Biology* **57**, 50-62 (2015); published online EpubJan (10.1111/jipb.12297).

15. G. K. Voeltz, M. M. Rolls, T. A. Rapoport, Structural organization of the endoplasmic reticulum. *EMBO Reports* **3**, 944-950 (2002); published online EpubJuly 23 (10.1093/embo-reports/kvf202).

16. L. R. Griffing, Networking in the endoplasmic reticulum. *Biochem Soc Trans* **38**, 747-753 (2010); published online EpubJun (10.1042/BST0380747).

17. S. A. Opeyemi, *Effect of hyperosmotic stress on the network morphology and transport function of the endoplasmic reticulum in tobacco*. A Senior Scholars Thesis, Texas A&M University.

18. R. W. Ridge, Y. Uozumi, J. Plazinski, U. A. Hurley, R. E. Williamson, Developmental transitions and dynamics of the cortical ER of *Arabidopsis* cells seen with green fluorescent protein. *Plant Cell Physiology* **40(12)**, 1253-1261 (1999).

19. Y. Shibata, T. Shemesh, W. A. Prinz, A. F. Palazzo, M. M. Kozlov, T. A. Rapoport, Mechanisms determining the morphology of the peripheral ER. *Cell* **143**, 774-788 (2010); published online EpubNovember 24 (10.1016/j.cell.2010.11.007).

20. B. E. S. Gunning, M. W. Steer, *Plant Cell Biology: Structure and Function*. (Jones and Bartlett Publishers, 1996).

21. N. Tolley, I. A. Sparkes, P. R. Hunter, C. P. Craddock, J. Nuttall, L. M. Roberts, C. Hawes, E. Pedrazzini, L. Frigerio, Overexpression of a plant reticulon remodels the lumen of the cortical endoplasmic reticulum but does not perturb protein transport. *Traffic* **9**, 94-102 (2008); published online EpubJan (10.1111/j.1600-0854.2007.00670.x).

22. G. K. Voeltz, W. A. Prinz, Y. Shibata, J. M. Rist, T. A. Rapoport, A class of membrane proteins shaping the tubular endoplasmic reticulum. *Cell* **124**, 573-586 (2006); published online EpubFeb 10 (10.1016/j.cell.2005.11.047).

23. I. Sparkes, N. Tolley, I. Aller, J. Svozil, A. Osterrieder, S. Botchway, C. Mueller, L. Frigerio, C. Hawes, Five *Arabidopsis* reticulon isoforms share endoplasmic reticulum location, topology, and membrane-shaping properties. *Plant Cell* **22**, 1333-1343 (2010); published online EpubApr (10.1105/tpc.110.074385).

24. K. Knox, P. Wang, V. Kriechbaumer, J. Tilsner, L. Frigerio, I. Sparkes, C. Hawes, K. Oparka, Putting the squeeze on plasmodesmata: A role for reticulons in primary plasmodesmata formation. *Plant Physiology* **168**, 1563-1572 (2015); published online EpubAug (10.1104/pp.15.00668).

25. U. Neumann, F. Brandizzi, C. Hawes, Protein transport in plant cells: in and out of the Golgi. *Ann Bot* **92**, 167-180 (2003); published online EpubAug (10.1093/aob/mcg134).

26. I. A. Sparkes, T. Ketelaar, N. C. de Ruijter, C. Hawes, Grab a Golgi: laser trapping of Golgi bodies reveals in vivo interactions with the endoplasmic reticulum. *Traffic* **10**, 567-571 (2009); published online EpubMay (10.1111/j.1600-0854.2009.00891.x).

27. L. R. Griffing, Plant and cell architecture. in *Plant Physiology and Development*. (Sinauer Associates, Inc., 2015), chap. 1, pp. 1-50.

28. A. R. English, G. K. Voeltz, Rab10 GTPase regulates ER dynamics and morphology. *Nature Cell Biology* **15**, 169-178 (2012); published online EpubDecember 23 (10.1038/ncb2647).

29. K. Anwar, R. W. Klemm, A. Condon, K. N. Severin, M. Zhang, R. Ghirlando, J. Hu, T. A. Rapoport, W. A. Prinz, The dynamin-like GTPase Sey1p mediates homotypic ER fusion in *S. cerevisiae*. *J Cell Biol* **197**, 209-217 (2012); published online EpubApr 16 (10.1083/jcb.201111115).

30. M. Zhang, J. Hu, Homotypic fusion of endoplasmic reticulum membranes in plant cells. *Front Plant Sci* **4**, 514 (2013); published online EpubDec 18 (10.3389/fpls.2013.00514).

31. M. Zhang, F. Wu, J. Shi, Y. Zhu, Z. Zhu, Q. Gong, J. Hu, ROOT HAIR DEFECTIVE3 family of dynamin-like GTPases mediates homotypic endoplasmic reticulum fusion and is essential for *Arabidopsis* development. *Plant Physiol* **163**, 713-720 (2013); published online EpubOct (10.1104/pp.113.224501).

32. J. Runions, T. Brach, S. Kuhner, C. Hawes, Photoactivation of GFP reveals protein dynamics within the endoplasmic reticulum membrane. *J Exp Bot* **57**, 43-50 (2006); published online EpubOctober 5 (10.1093/jxb/eri289).

33. L. Xiong, K. S. Schumaker, J.-K. Zhu, Cell signaling during cold, drought, and salt stress. *The Plant Cell* **14**, S165-S183 (2002); published online EpubMay (10.1105/tpc.000596).

34. P. S. Nobel, *Physicochemical and Environmental Plant Physiology*. (Elsevier Inc, ed. 4, 2009).

35. I. Lang, S. Sassmann, B. Schmidt, G. Komis, Plasmolysis: Loss of turgor and beyond. *Plants* **3**, 583-593 (2014); published online EpubNov 26 (doi:10.3390/plants3040583).

36. K. Hecht, Studien über den vorgang der plasmolyse. *Beiträge zur Biologie der Pflanzen* **11**, 133-189 (1912).

37. K. J. Oparka, D. A. M. Prior, J. W. Crawford, Behaviour of plasma membrane, cortical ER and plasmoldesmata during plasmolysis of *onion* epidermal cells. *Plant, Cell and Environment* **17**, 163-171 (1994); published online EpubFeb (10.1111/j.1365-3040.1994.tb00279.x).

38. I. Lang-Pauluzzi, The behaviour of the plasma membrane during plasmolysis: a study by UV microscopy. *Journal of Microscopy* **198**, 188-198 (2000); published online EpubJun (10.1046/j.1365-2818.2000.00677.x).

39. I. Lang-Pauluzzi, B. E. S. Gunning, A plasmolytic cycle: the fate of cytoskeletal elements. *Protoplasma* **212**, 174-185 (2000); published online EpubOct (10.1007/BF01282918).

40. M. Terasaki, Dynamics of the endoplasmic reticulum and golgi apparatus during early sea urchin development. in *Molecular Biology of the Cell*. (The American Society for Cell Biology, 2000), vol. **11**, pp. 897–914.

41. T. Hamada, H. Ueda, T. Kawase, I. Hara-Nishimura, Microtubules contribute to tubule elongation and anchoring of endoplasmic reticulum, resulting in high network complexity in *Arabidopsis*. *Plant Physiology* **166**, 1869-1876 (2014); published online EpubDec (10.1104/pp.114.252320).

42. J. Haseloff, K. R. Siemering, D. C. Prasher, S. Hodge, Removal of a cryptic intron and subcellular localization of green fluorescent protein are required to mark transgenic *Arabidopsis* plants brightly. *Proc. Natl. Acad. Sci.* **94**, 2122–2127 (1997); published online EpubMarch (10.1073/pnas.94.6.2122).

43. M. T. Ruiz, O. Voinnet, D. C. Baulcombe, Initiation and maintenance of virus-induced gene silencing. *The Plant Cell* **10**, 937–946 (1998); published online EpubJune (10.1105/tpc.10.6.937).

44. K. Ueda, T. Matsuyama, T. Hashimoto, Visualization of microtubules in living cells of transgenic *Arabidopsis thaliana*. *Protoplasma* **206**, 201-206 (1999); published online EpubJan (10.1007/BF01279267).

45. B. Schmid, ImageJ 3D Viewer. (2009), Retrieved from https://imagej.nih.gov/ij/plugins/3d-viewer/

46. Kitware, VTK (Visualization tool kit) (2016), Retrieved from http://www.vtk.org

47. L. C. Enloe, L. R. Griffing, Improved volume rendering for the visualization of living cells examined with confocal microscopy. *In Visual Data Exploration and Analysis VII* **3960**, (2000); published online EpubJan (10.1117/12.378915).

48. Adobe, Adobe illustrator (2016), Retrieved from https://http://www.adobe.com/products/illustrator.html

49. K. li, The image stabilizer plugin for ImageJ. (2008), Retrieved from http://www.cs.cmu.edu/~kangli/code/Image_Stabilizer.html

50. J. Hardin, FRAP profiler final plugin in ImageJ. (2016), Retrieved from http://worms.zoology.wisc.edu/research/4d/4d.html - frap

51. I. Lang, D. A. Barton, R. L. Overall, Membrane-wall attachments in plasmolysed plant cells. *Protoplasma* **224**, 231-243 (2004); published online EpubDec (10.1007/s00709-004-0062-6).

52. S. L. Shaw, R. Kamyar, D. W. Ehrhardt, Sustained microtubule treadmilling in *Arabidopsis* cortical arrays. *Science* **300**, 1715-1718 (2003); published online EpubJun 13 (10.1126/science.1083529).

53. D. Drobne, 3D imaging of cells and tissues by focused ion beam/scanning electron microscopy (FIB/SEM). in *Methods Mol Biol*. (2013), vol. **950**, chap. 16, pp. 275-292.

54. K. Narayan, S. Subramaniam, Focused ion beams in biology. *Nat Methods* **12**, 1021-1031 (2015); published online EpubNov (10.1038/nmeth.3623).

55. D. G. Mellersh, M. C. Heath, Plasma membrane–cell wall adhesion is required for expression of plant defense responses during fungal penetration. *The Plant Cell* **13**, 423-424 (2001); published online EpubFeb (10.1105/tpc.13.2.413).

56. C. Knepper, E. A. Savory, B. Day, *Arabidopsis* NDR1 is an integrin-like protein with a role in fluid loss and plasma membrane-cell wall adhesion. *Plant Physiology* **156**, 286-300 (2011); published online EpubMay (10.1104/pp.110.169656).

57. W. J. Lucas, Plasmodesmata: intercellular channels for macromolecular transport in plants. *Curr Opin Cell Biol* **7**, 673-680 (1995); published online EpubFeb (10.1016/0955-0674(95)80109-X).

58. J. Y. Lee, H. Lu, Plasmodesmata: the battleground against intruders. *Trends Plant Sci* **16**, 201-210 (2011); published online EpubApr (10.1016/j.tplants.2011.01.004).

59. G. Stefano, L. Renna, F. Brandizzi, The endoplasmic reticulum exerts control over organelle streaming during cell expansion. *J Cell Sci* **127**, 947-953 (2014); published online EpubMar 1 (10.1242/jcs.139907).

60. B. Kachar, T. S. Reese, The mechanism of cytoplasmic streaming in *characean* algal cells: sliding of endoplasmic reticulum along actin filaments. *J Cell Biol* **106(5)**, 1545-1552 (1988).

61. C. Van der Schoot, L. K. Paul, S. B. Paul, P. L. Rinne, Plant lipid bodies and cell-cell signaling: a new role for an old organelle? *Plant Signal Behav* **6**, 1732-1738 (2011); published online EpubNov (10.4161/psb.6.11.17639).

62. F. Cordeli, ImageJ Manual Tracking Plugin. (2005), Retrieved from http://rsbweb.nih.gov/ij/plugins/track/track.html

63. M. Tominaga, A. Kimura, E. Yokota, T. Haraguchi, T. Shimmen, K. Yamamoto, A. Nakano, K. Ito, Cytoplasmic streaming velocity as a plant size determinant. *Dev Cell* **27**, 345-352 (2013); published online EpubNov 11 (10.1016/j.devcel.2013.10.005).

64. I. F. Sbalzarini, A. Mezzacasa, A. Helenius, P. Koumoutsakos, Effects of organelle shape on fluorescence recovery after photobleaching. *Biophys J* **89**, 1482-1492 (2005); published online EpubSep (10.1529/biophysj.104.057885).

65. G. Stefano, C. Hawes, F. Brandizzi, ER - the key to the highway. *Curr Opin Plant Biol* **22**, 30-38 (2014); published online EpubDec (10.1016/j.pbi.2014.09.001).

66. A. Toulmay, W. A. Prinz, Lipid transfer and signaling at organelle contact sites: the tip of the iceberg. *Curr Opin Cell Biol* **23**, 458-463 (2011); published online EpubAug (10.1016/j.ceb.2011.04.006).